ANEXO 8 PUBLICACIONES DE LA TESIS

FUENTE **Natural Hazards**, Journal of the International Society for the Prevention and Mitigation of Natural Hazards. Glade Th, Murty TS, Schenk V (eds); ISSN 0921-030X (print version) 1573-0840 (electronic version). © SPRINGER Science+Business Media B.V.

Bulletin of Engineering Geology and the Environment, The official journal of the IAEG. Brian Hawkins (ed. in chief); ISSN 1435-9529 (print version) 1435-9237 (electronic version). © SPRINGER-Verlag

La tesis "Movimientos de Ladera en la Vertiente Meridional de Sierra Nevada (Granada, España): Identificación, Análisis y Cartografía de Susceptibilidad y Peligrosidad mediante SIG", se presenta bajo la modalidad de "agrupación de publicaciones". El presente anexo corresponde al original de las publicaciones que constituyen los capítulos 2, 3 y 4 de la tesis[5]. Asimismo, se incorpora un informe del factor de impacto y citas de la revista, e informe del ranking por categoría, según Thomson Reuters. Las publicaciones no se han presentado, ni se van a presentar, en otra tesis doctoral diferente. Se considera la idoneidad de la tesis bajo este formato ya que las publicaciones presentan una clara continuidad en la línea de investigación, satisfacen los objetivos propuestos y están concadenadas de forma que cada una constituye un capítulo de la tesis que marca el avance de la investigación.

[5] A las tres publicaciones incorporadas (a modo de capítulos de la tesis), se le añade un capítulo (aparte del introductorio y conclusiones) que amplia y completa el trabajo en clara continuidad con la investigación planteada.

Nat Hazards (2009) 50:571–590
DOI 10.1007/s11069-008-9305-8

ORIGINAL PAPER

Building models for automatic landslide-susceptibility analysis, mapping and validation in ArcGIS

J. D. Jiménez-Perálvarez · C. Irigaray · R. El Hamdouni · J. Chacón

Received: 29 October 2007 / Accepted: 10 October 2008 / Published online: 4 November 2008

Abstract In this paper, ModelBuilder™ in ArcGIS (ESRI) has been applied to landslide-susceptibility analysis, mapping and validation. The models (scripts), available for direct downloading as an ArcGIS tool, allow landslide susceptibility to be computed in a given region, providing a landslide-susceptibility map, with the GIS matrix method, and ensuring a quality validation. The paper details the steps needed for the model-building process, enabling users to build their own models and to become more familiar with the tool. The susceptibility model leads the user first through a Digital Elevation Model (DEM), depicting the morphological and morphometric features of the study area, and then through a Digital Terrain Model (DTM), useful as a source of landslide-determinant factors, such as slope elevation, slope angle and slope aspect. In addition, another determinant factor is the lithological unit, independent of the DEM. Once the determinant landslide factors are reclassified and in a vectorial format, all the combinations between the classes of these factors are determined using the geoprocessing abilities of ArcGIS. The next step for the development of the landslide-susceptibility model consists of identifying the areas affected by a given surface of rupture (i.e. source area) in every combination of the determinant-factor classes. This step leads to the landslide matrix based on a previously georeferenced landslide database of the region, in which the slopes are distinguished into two simple classes: with or without landslides. In the last stage, to build a landslide-susceptibility model, the user computes the percentages of area affected by landslides in every combination of determinant factors. In the resulting landslide-susceptibility map a progressive zonation of areas or slopes increasingly prone to landslides is performed. A model for the

J. D. Jiménez-Perálvarez · C. Irigaray (✉) · R. El Hamdouni · J. Chacón
Department of Civil Engineering. ETSICCP, University of Granada, Spain, Campus Fuentenueva s/n, Granada 18071, Spain
e-mail: clemente@ugr.es

J. D. Jiménez-Perálvarez
e-mail: jorgejp@ugr.es

R. El Hamdouni
e-mail: rachidej@ugr.es

J. Chacón
e-mail: jchacon@ugr.es

validation of the resulting landslide-susceptibility map is also presented, based on the determination of the degree of fit, which is calculated from the cross tabulation between a set of landslides (not included in the susceptibility analysis) and the corresponding susceptibility map.

Keywords Bivariate statistical analysis · Landslide susceptibility · GIS matrix method · ArcGIS

1 Introduction

Landslides (slope movements) are natural or man-induced phenomena that generate risks (Varnes 1984; Fell 1994; Glade et al. 2005; Chacón et al. 2006), and therefore it would be necessary to consider such processes in land-use planning. Unfortunately, slope movements are commonly taken into account only in *post mortem* analyses of catastrophic events, or for civil engineering purposes (Varnes 1978; Chacón et al. 2006).

Landslide susceptibility, a measure of how prone land units are to landsliding, was quantitatively approached by Brabb et al. (1972). In mathematical form, it can be expressed as the probability of spatial occurrence of slope failures, given a set of geoenvironmental conditions (Guzzetti et al. 2005). In general, susceptibility can be evaluated by two methods: (1) those based on modelling techniques founded on physical and mechanic laws of the equilibrium of forces, and (2) those based on statistical techniques founded on the principle of actualism, in which the GIS can be of great utility. Geographical Information Systems (GIS) offer a powerful tool for analysing the processes which occur on the Earth's surface (Bonham-Carter 1994). The availability of personal computers and the great number of commercial GIS software packages favoured a widespread use of GIS for the analysis and modelling of georeferenced data, and the development of specific applications for physical processes such as slope instability (Carrara et al. 1995; Irigaray 1995; Ayalew and Yamagishi 2005; Chacón et al. 2006; Davis et al. 2006).

Methods for GIS landslide-susceptibility mapping evolved over time, taking into account different significant contributions (Crozier 1986; Carrara et al. 1991; Chung et al. 1995; Canuti and Casagli 1996; Guzzetti et al. 1996; Soeters and Van Westen 1996; Aleotti and Chowdhury 1999; Iovine et al. 2003a, b) and the increasing worldwide experience on GIS landslide mapping (Chacón et al. 2006). According to Van Westen et al. (1997) and Van Westen (2000) in the analysis of susceptibility in GIS, several methodologies can be differentiated into:

- the empirically based approach, particularly suited for small-scale regional surveys. It relies on the production of landslide-hazard maps investigated and controlled by the earth scientist responsible for the analysis (heuristic qualitative approach) (Carrara and Merenda 1974; Stevenson 1997; Kienholz et al. 1983).
- the statistical quantitative approach for medium-scale surveys or inventory-based method (also empirically based). It allows for a better comprehension of the relationships between landslides and preparatory factors, and guarantees lower subjectivity levels with respect to the heuristic approach (Ermini et al. 2005). In the statistical analysis, the combinations of factors that led to landslides in the past are determined statistically, and quantitative predictions can be made for areas currently free of landslides, in which similar conditions exist. Notable within the statistical methods are basically multivariate and bivariate statistics.

- the data-driven multivariate statistical analysis. All the parameters at unstable sites are analysed by multiple-regression techniques; alternatively, parameter maps are crossed with landslide-distribution maps, and the correlation is established for stable and unstable areas by employing discriminant analyses. One of the pioneer works was that of Carrara et al. (1977), which was continued by other works (Carrara 1988; Carrara et al. 1992, 1995; Chung et al. 1995).
- the experience-driven bivariate statistical analysis, based on indirect mapping. In this method, the causal factors are entered into a GIS and crossed with a landslide-distribution map. There are different varieties of this method, notably the weights of evidence (Bonham-Carter et al. 1988; Agterberg et al. 1989, 1993; Poli and Sterlacchini 2007), the landslide-index method (Van Westen 1993, 1994; Van Westen et al. 1997) and the one used in the present work, the matrix method (DeGraff and Romesburg 1980; Maharaj 1993; Cross 1998; Irigaray 1995; Irigaray et al. 1999, 2007; Clerici et al. 2002).

– the physically based or process-based approach for detailed studies. These consist of slope-stability analyses generally aimed at evaluating a safety factor (Okimura and Kawatani 1986; Mulder and Van Asch 1988; Hammond et al. 1992; Pack et al. 1998).

As a whole, a high number of GIS landslide-susceptibility (or hazard) methods were developed (Carrara et al. 1995; Guzzetti et al. 1999). Nevertheless, susceptibility maps need to be validated. Through validation (sometimes called evaluation or test), the quality of the proposed susceptibility estimate must be evaluated (Irigaray et al. 1999, 2007; Chung and Fabbri 2003; Guzzeti et al. 2006). The quality of a landslide-susceptibility model can be ascertained using the same landslide data used for the estimate, or by using independent landslide information not employed for the assessment (Guzzetti et al. 2006). Three basic techniques can be used to obtain an independent sample of landslides for validating a landslide-susceptibility map (Remondo et al. 2003): (a) the original inventory can be randomly split into two groups, one for the susceptibility analysis and one for validation; (b) the analysis can be conducted in a part of the study area, and the susceptibility map tested in another part (i.e. affected by different landslides); (c) the analysis can be made using landslides generated in a certain period, and validation performed by considering landslides occurred in different periods. The latter technique, used in the present work, is considered to be the most reliable technique to test the validity of the prediction made (Irigaray et al. 2007).

The currently available commercial GIS packages include programming tools and graphic interfaces which enable the user to rapidly design their own geoprocessing applications. “Model Builder” is a programming tool developed by ESRI (ArcGIS 2004), added to the GIS suite of packages since ArcView 3.0, which includes geoprocessing tools for the generation of recyclable models (McCoy 2004).

The main intention of the paper is the presentation of ArcGIS implemented geoprocessing models (scripts) based on ESRI’s “Model Builder” utility for automatic landslide-susceptibility analysis, using a validated methodology: the GIS matrix method (GMM). The latter offers a good opportunity to GIS users to conduct simple, inventory-based landslide-susceptibility analyses within a familiar commercial GIS environment. Different public organisms (ministries, city halls, research centres) have databases on slope movements that are continuously updated. The proposed landslide-susceptibility model, described in this work, can employ such updated databases in order to validate and revise susceptibility maps with the aim of incorporating them in territorial ordination plans. The tool is available for free downloading as an ArcGIS tool (see details in Appendix).

For the application and activation of the models, a study area characterized by a considerable incidence of landslides was selected (El Hamdouni 2001; Fernández 2001; Chacón et al. 2002; Jiménez-Perálvarez et al. 2005; Chacón et al. 2006; Irigaray et al. 2007). The area (Fig. 1) is located on the southern slopes of Sierra Nevada, in the Betic Cordillera (Spain), with an approximate extent of 158 km^2. In the area the units of the Internal Zones of the Betic Cordillera and post-tectonic materials (Neogene and Quaternary) outcrop. In this sector, the Internal Zone is represented by the Alpujarride and Nevado-Filabride Complexes. Dark schist and feldspar-bearing micaschist are widespread in the Nevado-Filabride Complex up to the Alpujarride Complex, which is composed of Triassic calcareous schist, marble, phyllite and quartzite (Gómez-Pugnaire et al. 2004). The Neogene materials are composed of marl and silt covered by conglomerate (Ortega et al. 1985).

2 Foundations of the models and of required data

The landslide-susceptibility model presented in this work (tool: "susceptibility_model") is based on the GMM, which is a GIS-based method developed by improving a previous method (DeGraff and Romesburg 1980), contributed by Irigaray (1995). In the empirical analysis, an assumption is made that future landslides will occur under the same conditions as in the past. The method is based on bivariate statistical analysis, in turn, founded on cross analysis of maps of determinant factors and spatial frequency of slope movements. It permits an evaluation of the instability index in a given zone, although it is not capable of predicting the susceptibility to slope movements in terms of absolute probability. However, it enables to evaluate the potential relative instability in a broad region by using a series of measurable factors.

The GMM is an appropriate methodology for the working scale of this work (Van Westen et al. 1997). The GMM requires an inventory of landslides and a selection of the most significant determinant factors to be included in the analysis. The determinant factors

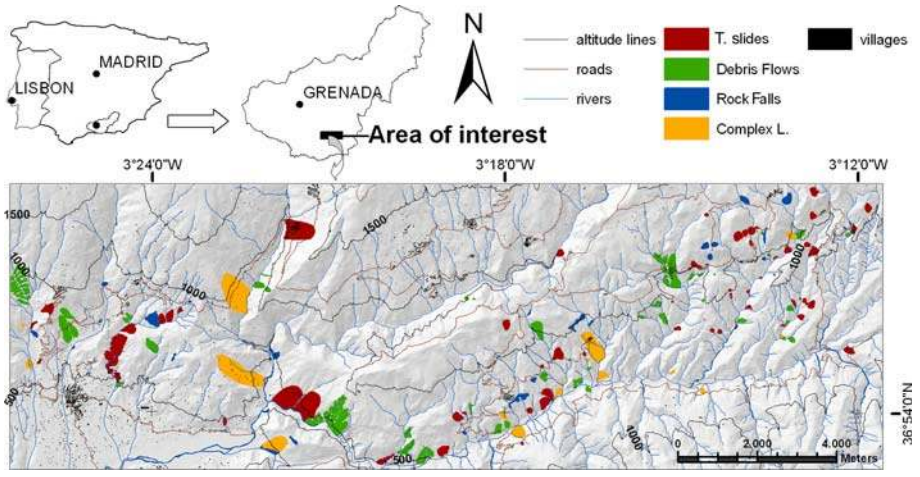

Fig. 1 Location and landslide inventory map. The landslide inventory is composed of 69 translational slides, 52 debris flows, 31 rock falls and 17 complex slides

are not weighted: the weighting factors are in fact intrinsically performed by the matrix method, as described by different authors (Maharaj 1993; Cross 1998; Irigaray et al. 1999, 2007; Clerici et al. 2002; Fernández et al. 2003). It was also validated with excellent results in the same region where the study area is located (Irigaray et al. 1999, 2007; El Hamdouni 2001; Fernández 2001; Fernández et al. 2003). A quantitative comparison between the GIS matrix method and other bivariate statistical-analysis techniques (Landslide Susceptibility Index—Van Westen 1993, 1994; and weight of evidence—Bonham-Carter 1994) is presented in Sect. 3.5.

2.1 Landslide inventory

When adopting a statistical probabilistic approach, the landslide inventory is the first step in any landslide-mapping project intended to provide a susceptibility, hazard or risk assessment. It is perhaps the most important set of data in the entire assessment process and greatly influences the quality of the final results.

In this study, a database containing 169 landslides, described with internationally accepted terms and classifications (Varnes 1978; Cruden and Varnes 1996), was first implemented by collecting data gathered through a phase of interpretation of aerial photographs (at scale 1:20,000) followed by field surveying. The definitive inventory of slope movements was made at a scale of 1:10,000. This landslide inventory is based on movements generated before 1996. The inventory includes a total of 69 slides (translational slides, mainly in phyllite and marble), 52 flows (debris flows, mainly in phyllite), 31 falls (rock falls, mainly in marble) and 17 complexes (complex slides, mainly in quartzite), all identified and mapped (Tables 1, 2 and Fig. 1). The landslides, considered from the source areas to the deposits, were found to affect 3.79% of the total study area. Phyllite units resulted to be the most unstable materials, comprising 38% of the inventoried landslides, followed by marble units at 25%.

2.2 Determinant factors

The determinant factors account for the overall slope-stability condition: the strength of the geological units can in fact be related to the type of soil or rock, to discontinuities or to slope morphology in terms of slope angle, aspect, elevation, size, amplitude (surface covered by a homogeneous slope unit with slope aspect approximately uniform), roughness (describes different combinations of slope angle and aspect in a given region), curvature (describes the slope profile and differences between concave and convex profiles), etc.

Table 1 Landslide inventory, typologies and dimensions

Affected area (m^2)						
Typology	*n*	Maximum	Minimum	Mean	Total	% Relate to total area
Slide (translational slide)	69	686,172	232	37,484	2,661,346	1.68
Flow (debris flow)	52	355,198	287	40,088	2,084,598	1.32
Fall (rock fall)	31	64,244	453	12,792	396,557	0.25
Complex	17	462,465	3,547	57,849	867,741	0.55
Total	169	686,172	232	35,564	6,010,241	3.79

Table 2 Landslide inventory, percentages in each lithology

% of landslides inventoried in each LITHOLOGY relate to total lithologies of each typology							
Typology	Cs.	Cgm.	Qtze.	Scht.	Marb.	Mscht.	Pht.
Slide (translational slide)	9.86	9.86	18.31	0.00	22.54	0.00	39.44
Flow (debris flow)	0.00	1.92	21.15	5.77	0.00	9.62	61.54
Fall (rock fall)	6.45	0.00	3.23	16.13	74.19	0.00	0.00
Complex	0.00	0.00	40.00	0.00	26.67	6.67	26.67
Total	4.14	4.73	18.93	5.33	24.85	4.14	37.87

Cs Calcareous schist; *Cgm* Conglomerate; *Qtze* Quartzite; *Scht* Schist; *Marb* Marble; *Mscht* Micaschist; *Pht* Phyllite

The model presented in this paper uses four determinant factors: three DEM derivatives (slope angle, slope elevation and slope aspect), and one derivative from a thematic GIS layer (lithology). Among these factors, those ones most frequently considered in the international literature are slope angle and lithology (Rodríguez-Ortiz et al. 1978; Hansen 1984; Crozier 1986; Guzzetti et al. 1996, 1999; Irigaray et al. 1996, 1999, 2007; Fernández et al. 2003; Ayalew and Yamagishi 2005).

In the study zone, an exhaustive analysis of the most relevant determinant factors was recently published (Irigaray et al. 2007). Even so, with the aim of selecting the set of significant determinant factors, an analysis was performed by crossed tabulation (contingency tables) between the source areas of the landslides and determinant factors. Different correlation coefficients were calculated and significance tests were used to identify the most influencing factors: Chi-square, Coefficient of linear correlation of the contingency coefficient, Tschuprow's T and Cramer's V coefficients (Table 3). Those determinant

Table 3 Correlation between the source areas of the landslides and the determinant factors

Factor	χ^2	*R*	*T*	*V*
AL	6.27	0.40	0.07	0.12
IL	3.51	0.35	0.06	0.09
LC	1.20	0.27	0.05	0.05
VC	1.12	0.26	0.03	0.05
FT	0.25	0.18	0.02	0.02
SA	6.80	0.41	0.09	0.12
PP	2.06	0.31	0.05	0.07
LT	12.95	0.48	0.10	0.17
W	0.32	0.19	0.03	0.03
LU	0.46	0.21	0.02	0.03
SL	6.75	0.41	0.09	0.12

Lithology, slope angle, slope aspect and altitude are the determinant factors which show the highest degree of association

AL Altitude; *IL* Illumination; *LC* Lithological contacts; *VC* Vertical curvature; *FT* Faults; *SA* Slope aspect; *PP* Precipitation (annual mean); *LT* Lithology; *W* Distance to watercourses; *LU* Land use; *SL* Slope angle; χ^2 Chi-Square; *R* Lineal and contingency correlation coefficient *C* $R = \sqrt{(C/C_{\max})}$; T Tschuprow's *T*; V Cramer's *V*

factors showing the highest degree of association with the landslide inventory were then taken into consideration: lithology, slope angle, slope aspect and altitude (or elevation).

The determinant factors of instability can vary according to the study zone. In each area, those factors which show the highest degree of association with the landslide inventory should be selected. The model can be easily edited in order to add any other determinant or triggering factor. In this case, previous results (El Hamdouni 2001; Fernández 2001) concerning the reclassification of the determinant factors were adopted, and an entire numerical value was assigned to each class of determinant factors, although further developments of the model could be improved by using other classification methods (natural-breaks, standard deviation, equal intervals, etc.) (Irigaray et al. 2007).

Slope elevation is not the most common determinant factor in the literature, except for studies of mountain areas (like the study area) with pronounced differences in elevation (Fernández et al. 2008). Usually, elevation is considered as an indirect factor, related to/or conditioning other factors such as rainfall, temperature, freeze/thaw cycles, soil development, vegetation, etc., which may be more difficult to quantify. In the zone, the elevation varies between 300 and 1800 m, representing an interval wide enough to introduce significant changes in such climatic conditions such as rainfall and temperature, and also a variable set of vegetation units. The slope angle is one of the most commonly used determinant factors in GIS applications concerning slope-stability (Fernández et al. 2008). The slope aspect (or exposition) has only an indirect influence on landsliding. It is related to other variables, such as soil moisture and development, weathering, etc., which are commonly more intense on north-oriented slopes, because of the lower insolation. Lithology is the most common determinant factor in most stability studies. The model (tool) presented here requires the lithology map as an input datum in order to evaluate the landslide susceptibility. It represents the strength of the materials in terms of slope behaviour during landslides or instability processes. From the Mining and Geology Information System of Andalusia (Spain) (SIGMA 2002), the 1:50,000 geological map of the region was drawn. With the recommendations on map use in geological engineering projects of UNESCO (1976), a number of lithological complexes were reclassified in the units shown on the source map (Fig. 2).

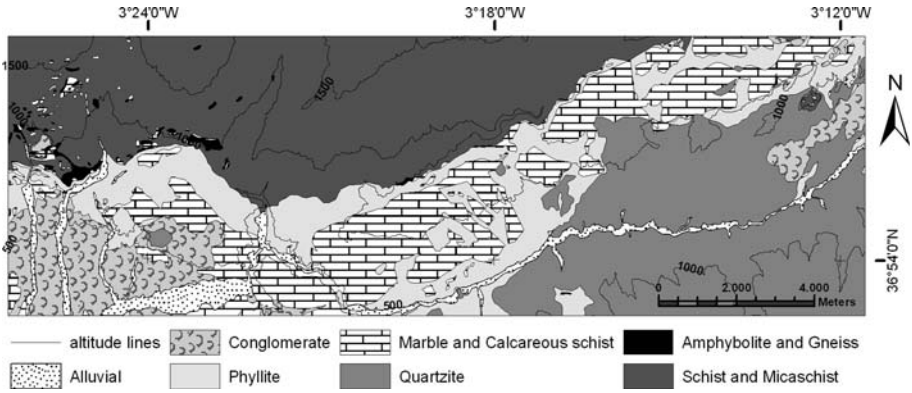

Fig. 2 Lithological complex map

2.3 Method of analysis: the GIS matrix method

Once the relevant determinant factors are identified, the landslide susceptibility can be evaluated by delimiting terrain units differently prone to landslides. The GMM was successfully applied to different geological settings and countries (Irigaray 1995; Cross 1998; Irigaray et al. 1999, 2007; Fernández 2001; El Hamdouni 2001). It is based on the computation of three matrices: landslide matrix (LM), total surface of the study area matrix (TSM), and susceptibility matrix (SM). First, a LM is established by calculating areas or extensions affected by the source areas of the landslides in each combination of classes of the selected determinant factors. The TSM matrix is calculated by making all the possible combinations among the classes of determinant factors selected, and then calculating the area occupied by each combination. Finally, in the SM, each cell shows a value calculated by dividing the value of the cell in the LM by the value of the cell in the TSM. The cell values in the SM represent an assessment of relative susceptibility corresponding to each combination of determinant factors in the cell. Each SM value shows the percentage of source areas in each combination of determinant factors with regard to the total area occupied by the respective combination of determinant factors. The susceptibility maps are based on 5 levels of classification, automatically assigned to each zone by using the natural-breaks method (Irigaray et al. 2007; ArcGIS 2004). In this method, class breaks are determined statistically by finding adjacent feature pairs which show relatively large differences in data value (ArcGIS 2004).

2.4 Validation of susceptibility maps

The landslide-susceptibility validation model presented in this work (tool: "validation_model") uses the *degree of fit* to assess the association between the inventory and the landslide-susceptibility map. The quality of the maps was assessed by techniques of spatial autocorrelation and measuring the *degree of fit* between a given set of data and the maps (Goodchild 1986). The final aim was to assess the quality of the susceptibility map as a predictive tool to explain the landslide inventory of the study area. Only when a given level of quality was attained, a given landslide susceptibility or hazard map may be considered acceptable as a predictive tool for future landslides. There are different approaches (Irigaray et al. 1999; Remondo et al. 2003; Guzzetti et al. 2006), and excellent results were achieved in landslide areas of the Betic Cordillera (Irigaray et al. 1999, 2007; El Hamdouni 2001; Fernández 2001; Fernández et al. 2003). In this paper a different inventory (i.e. not the one employed for computing the susceptibility map) was used for validation. However, a validation with the inventory map used to derive the landslide-susceptibility map was also made (Sect. 4.3). The *degree of fit* (DF), as applied to landslide maps, is defined as follows:

$$\mathrm{DF}_i = \frac{m_i/t_i}{\sum m_i/t_i}$$

where m_i is the area occupied by the source areas of the landslides at each susceptibility level i, and t_i is the total area covered by that susceptibility level. The *degree of fit* for each susceptibility level represents the percentage of mobilized area located in each susceptibility class. The lower the *degree of fit* (less than 7%) in the low and very low susceptibility classes (relative error), and the higher the *degree of fit* in the high or very high susceptibility classes (relative accuracy), the higher the quality of the susceptibility map will be (Fernández et al. 2003; Irigaray et al. 2007).

The selected set of source areas of the landslides for this validation is composed of 12 slides (translational slides, mainly in phyllite and marble), 6 flows (debris flows, mainly in phyllite), 1 fall (rock fall in marble) and 3 complexes (complex slides, mainly in quartzite). The landslides are homogeneously distributed in the study zone (Fig. 3) and reach 17.9% of the total surface covered by the set of source areas of the landslides considered for the LM calculation.

The landslide inventory used for the validation of the susceptibility map, is based on movements generated in the 1996–1997 winter season, as a consequence of heavy rains in the study area in late 1996 and early 1997 (212 mm in November 1996, 386 mm in December and 222 mm in January 1997, i.e. the mean annual rainfall for the area reached in only three months). The heavy rains damaged mainly the road network of the study zone (Irigaray et al. 2000).

3 The model for landslide-susceptibility mapping (susceptibility_model): input data, methodology and results

A model based on the assessment of landslide susceptibility was developed following the GMM. The model is inside the tool "susceptibility.tbx" and its name is "susceptibility_model".

3.1 Input data

Three input data are required for mapping the landslide susceptibility automatically: the DEM, the lithological map of the study area and the landslide inventory.

The DEM has to be a continuous raster surface or map. There are different techniques to determine DEMs from vectorial data, (IDW, Kriging, etc.), although there are high-quality DEMs supplied by public or commercial sources. The DEM of the present study is made by regular matrices with a pixel resolution of 10 × 10 m, achieved by transforming a TIN (Triangulated Irregular Network) to GRID. The TIN was generated from interpolation of digital contour lines and elevation points taken from a map at scale 1:10,000 (Andalusia Institute of Cartography; ICA 1999).

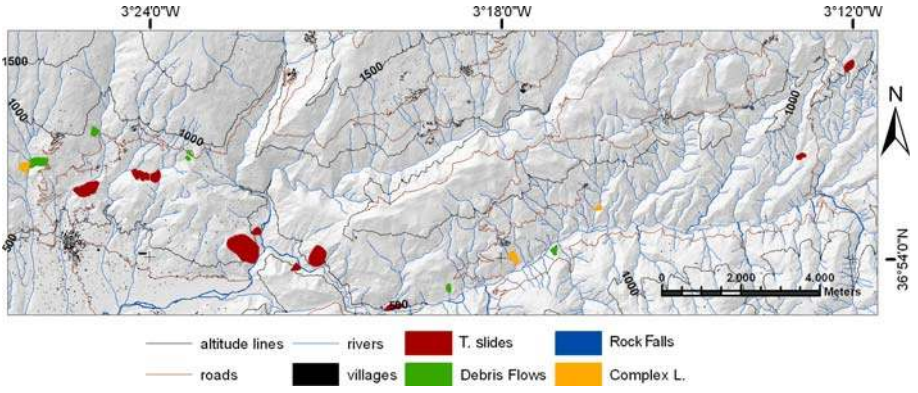

Fig. 3 Landslide inventory used for the validation of the landslide-susceptibility map. The inventory is composed of 12 translational slides, 6 debris flows, 1 rock fall and 3 complex slides

The lithological map has to be a vectorial layer showing a classification of lithological units. Each lithological complex has to be associated with an integer number.

The landslide inventory has to be a vectorial layer reclassified in two classes: presence of source areas of the landslides ("value_2"), or their absence ("value_1"). The sum of these two classes gives the total surface of the study area.

3.2 Modelling the matrix of the total surface of the study area (TSM)

From the DEM, three terrain digital models were derived as by-products showing three determinant factors: elevation, slope angle, and slope aspect (by means of the ArcGIS geoprocessing tools "Reclassify", "Slope" and "Aspect", resp.). The determinant factors expressed in raster format were reclassified and transformed into a vectorial format, and were generalized by classes, in order to attain a simpler attribute table for the map. These ArcGIS tools work in a raster format, which is necessary for the spatial analysis. Nevertheless, to improve the presentation of the data and reduce the size of the files, the three layers or maps (elevation, slope angle and slope aspect) were transformed from raster into vectorial format (".shp"). The maps were transformed into a vectorial format in order to work with different attribute layers. In the ArcGIS 9.0 version, it is not possible to edit attribute tables from raster maps. Each pixel in a raster map has that value in the vectorial map: afterwards it is homogenized to have in the attribute table a number of files equal to the number of map classes. The transformation of the format did not result in any loss of information. The fourth determinant factor, lithology, was introduced as parameter or input data, and each lithological complex was associated with an integer number. The TSM was computed by making all the possible combinations among all the classes of determinant factors selected by means of the ArcGIS geoprocessing tool "Intersect". Afterwards, a new column was added ("value") to the TSM generated layer. The value of this column is a simple identifier which was necessary to compute the TSM as a table, making further unions with other tables possible.

3.3 Modelling the landslide matrix (LM)

The LM was calculated by crossing the reclassified landslide inventory with the TSM by means of the ArcGIS geoprocessing tool "Tabulate Area". The results are shown in table "crossed.dbf", with three columns: "value", previously added from the TSM and corresponding to the identifier of each combination of classes of the determinant factors selected, "value_2" with the area affected by the source areas of the landslides in each combination, and "value_1" with the area not affected in each combination. The column "value_2" with the layer "intersect.shp" is, properly speaking, the LM (Sect. 2.3).

3.4 Modelling the susceptibility matrix (SM)

With the purpose of calculating the percentage of area affected by the source areas of the landslides in each of the classes of determinant factors, two new columns were generated in the LM table ("crossed.dbf"). The first column is the total area occupied by each of the combinations of classes of determinant factors selected. The second column is, in percentages, the area affected by the source areas of the landslides in each of the combinations of classes of determinant factors cited above. The column "value" of the table "crossed.dbf" shows the identifier of each combination, and coincides with the identifier "FID"

in the layer "intersect.shp", where each combination of factors may be seen in the different columns "GRIDCODE". By means of the ArcGIS geoprocessing tools "Make Feature Layer", "Add Join" and "Copy Features", the model links SM with the map or layer obtained by combining all the factors ("intersect.shp", which has the SM as an attribute table) in order to achieve a spatial representation of the area affected by the source areas of the landslides. This is the spatial presentation of the SM ("suscep_matrix.shp") with an attribute, a table composed of a series of columns. In column "crossed_po" the percentage of area affected by the source areas of the landslides in that factor combination is preserved, this being the corresponding susceptibility value.

3.5 Results

The output datum of the "susceptibility_model" is a vectorial layer: "suscep_matrix.shp". This layer is the result of the analysis, i.e. the landslide-susceptibility map. The susceptibility values varied between 0 and 100 in each combination of classes of determinant factors (one hundred in rows). The values obtained were visualized by means of 5 susceptibility levels (very low, low, moderate, high and very high) (Fig. 4, Table 4) found in surrounding areas (Irigaray 1995; Irigaray et al. 2007; El Hamdouni 2001; Fernández et al. 2003, 2008) using the natural-breaks method. In this example, a reclassification of natural-breaks was made (rounded off to the closest whole number). In this way, the classes distinguished were:

- Very low susceptibility: the affected area in a given combination of determinant factors extends between 0 and 1%.
- Low susceptibility: the affected area in a given combination of determinant factors extends between 1 and 5%.
- Moderate susceptibility: the affected area in a given combination of determinant factors extends between 5 and 15%.
- High susceptibility: the affected area in a given combination of determinant factors extends between 15 and 25%.
- Very high susceptibility: the affected area in a given combination of determinant factors extends above 25%.

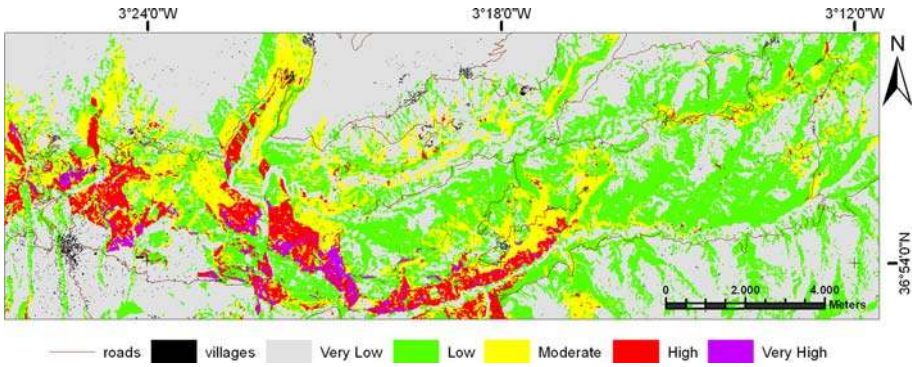

Fig. 4 Landslide-susceptibility map. The values are visualized showing 5 susceptibility levels found in surrounding areas using the natural-breaks method (Irigaray et al. 2007)

Table 4 Landslide susceptibility by different methodologies

Susceptibility	%	% Accumulate	km^2
Area (GIS matrix method)			
Very low	49.19	49.19	77.89
Low	30.51	79.7	48.31
Moderate	13.5	93.2	21.38
High	5.18	98.38	8.2
Very high	1.62	100	2.57
Area (weight of evidence method)			
Very low	35.71	35.71	56.56
Low	28.76	64.47	45.55
Moderate	20.64	85.11	32.7
High	10.45	95.56	16.56
Very high	4.43	100	7.02
Area (landslides-susceptibility Index method)			
Very low	45.32	45.32	71.78
Low	27.02	72.34	42.8
Moderate	15.42	87.75	24.42
High	8.7	96.45	13.78
Very high	3.54	100	5.61

The values show the surface area and percentages of each susceptibility level in relation to the whole area of study

The susceptibility values refer to slope instability or landslides without specifying the type of landslide. This may be adequate only for an initial susceptibility zonation, while detailed studies on the subject should consider susceptibility values found for each type of landslide (Chacón et al. 1996, 2006). The low and very low susceptibility levels represent more than 75% of the surface area studied. If moderate susceptibility is also added, this percentage rises to more than 90%. These values indicate that the maps obtained are not conservative, but rather they limit the zones of maximum susceptibility just to the relatively reduced area where the associated combination of factors exists.

Various bivariate-statistical techniques were applied on various mapping units. When comparing these results with those found by applying other susceptibility-analysis methods based on bivariate statistical techniques—Landslide Susceptibility Index (Van Westen 1993, 1994; Van Westen et al. 1997) and weight of evidence (Bonham-Carter 1994)—we found that the matrix method (GMM) is the least conservative of the methods considered (Fig. 5, Table 4). The zone considered by the GMM as exposed to high and very high susceptibility occupies a less area than the corresponding zones found by the other two methods. However, the validation of the susceptibility map by GMM is of the same nature as that made by the other methods (Fig. 6).

4 The model for landslide-susceptibility validation (validation_model): input data, methodology and validation

A model based on the assessment of the *degree of fit* between the source areas of the landslides and susceptibility zonation was developed following previous concepts and results (Goodchild 1986; El Hamdouni 2001; Fernández 2001; Fernández et al. 2003;

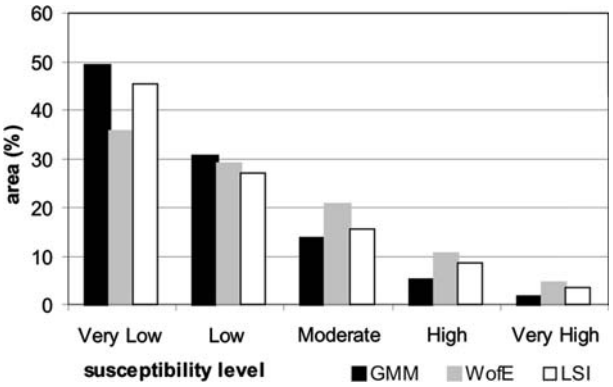

Fig. 5 Landslide-susceptibility by different methodologies. GMM, GIS matrix method; WofE, weight of evidence; LSI, landslide-susceptibility index. The values show the percentage of each susceptibility level in relation to the whole area of study

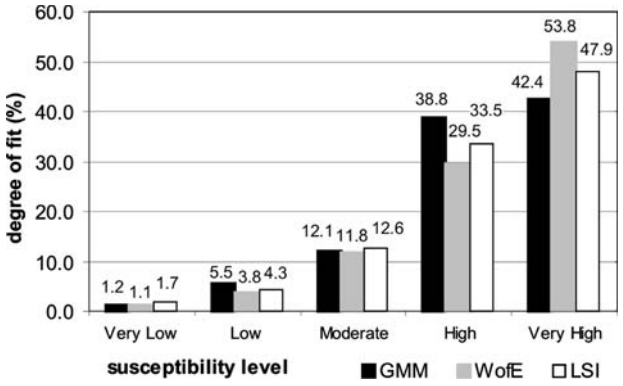

Fig. 6 Landslide-susceptibility map validation. Degree of fit between the source areas of the landslides and each landslide-susceptibility level. GMM. GIS, matrix method; WofE, weight of evidence; LSI, landslide-susceptibility index

Irigaray et al. 1999, 2007). The model is inside the tool "susceptibility.tbx" and its name is "validation_model".

4.1 Input data

Two separate sets of input data are necessary for the landslide-susceptibility validation: the landslide susceptibility map and a landslide inventory of the study area containing sources not employed for the susceptibility analysis.

The landslide-susceptibility map has to be the vectorial layer previously calculated by means of the "susceptibility_model": "suscep_matrix.shp".

The landslide inventory has to be a vectorial layer reclassified in two classes: presence of source areas of the landslides ("value_2"), or their absence ("value_1").

4.2 Modelling the validation of the landslide-susceptibility map

The validation model uses ArcGIS geoprocessing tools previously applied to the calculation of the *degree of fit* (*mi*, *ti*, etc.). The area affected by the source areas of the landslides in each susceptibility model (*mi*) (very low, low moderate, high and very high) is calculated by crossing the SM with the landslide inventory (binary map) used for the validation. As mentioned above, this inventory map must be different from the one employed for computing the SM. In addition, an additional validation phase was performed by considering the inventory map used for deriving the landslide-susceptibility map. As the SM includes a high number of rows, the SM was transformed into raster format and reclassified in the set of susceptibility classes previously selected: very low, low, moderate, high and very high. This reclassified map was crossed with the landslide inventory. Once the cross tabulation was established, new fields were added and calculated with values of *mi*, *ti*, *mi/ti*, etc. The operation (Σ(mi/ti)) was calculated by means of the ArcGIS geoprocessing tool "Summary Statistics", which may later be added ("Add Join") to the required calculations.

4.3 Landslide-susceptibility validation

The output datum of the "validation_model" is the table "adjust.dbf", i.e. the result of the landslide-susceptibility validation (Fig. 7). The obtained results clearly show a better degree of fit for the validation which was made with the inventory used to analyse the landslide-susceptibility map. However, it also shows a good degree of fit for the "true" validation inventory. The degree of fit for the very low and low susceptibility classes is 6.7%, which is similar to values reported in other works previously made in the same study zone (Irigaray et al. 1999, 2007; El Hamdouni 2001; Fernández 2001; Fernández et al. 2003). This error is due to the accumulated error in the technique (Irigaray et al. 2007), mainly due to the determining factors. This would be explained by the limitation of the method in terms of the DEM capability to express high slopes where the rock falls really occur. The scale of the geological map is generally less than the digitalization scale of the slope movements, and therefore a contact can assign an erroneous lithology to a movement.

5 Discussion and conclusions

The landslide-susceptibility maps are preventive tools intended to minimize risks in the threatened areas. Because of the social and economic implications in risk prevention, a key question is the quality of the maps, which derives from an appropriate procedure and can be tested through a proper validation. The tool presented here offers an automatic process of landslide-susceptibility mapping and validation; therefore, it allows to reduce the time-consuming process of development of GIS applications to landslide-susceptibility mapping and validation. The obtained results pointed out the quality of the maps drawn by means of the GMM in comparison with those made by other bivariate-statistical techniques. In general, the GMM effectively explains the spatial distribution of slope movements that took place after the drawing of the maps. Once the landslide susceptibility map is drawn and validated, it is possible to make a simple and quick selection of the most appropriate terrains for the setting of civil engineering or of building projects, or of areas where more detailed studies would be necessary. Nevertheless, it is vital to emphasize the crucial

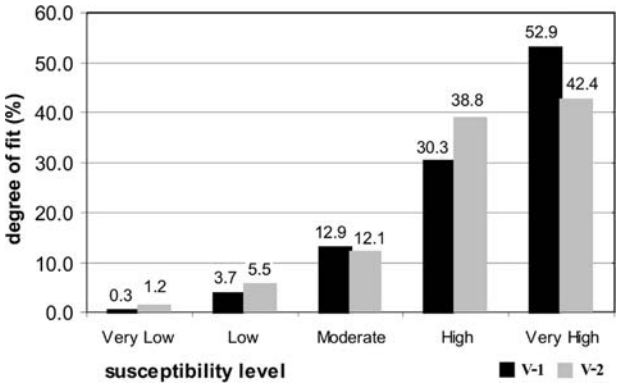

Fig. 7 Landslide-susceptibility map validation. Degree of fit between the source areas of the landslides and each landslide-susceptibility level. A comparison by using the inventory used to analyse the landslide-susceptibility map (V-1) and the new landslide inventory (V-2)

influence of an adequate engineering-geology approach, as well as of field and remote sensing surveys, in order to compile the basic data for landslide prevention: the inventory of landslides, the thematic layers related to the determinant factors and also all the available information on landslide-triggering factors.

The landslide susceptibility and the determinant factors involved in instability differ for each landslide type. In the example presented in this paper, all the landslide types were considered as a whole, and therefore the resulting landslide-susceptibility map was not derived from any particular type of landslide but rather from the overall inventory. This may be adequate only for an initial susceptibility zonation, while a more detailed susceptibility map should be prepared by processing separately the landslides by typologies, and using as input and validation inventories only those in each group or typology. In this paper, the basic data in the inventory are the source areas related to each landslide, this being appropriate for detailed scale maps (1:10,000 to 1:25,000). Nevertheless, at smaller scales, or regional mapping (1:25,000 to 1:400,000), it is possible to use the whole landslide areas as the basic input data in the landslide inventory: in fact, the purpose of low-detail maps is a more approximate indication of unstable zones than a precise location of areas potentially affected by new source areas.

Acknowledgements Work supported by CGL2005-03332 and CGL2008-04854 Projects. RNM121 Research Group and the Andalusian Excellence Project P06-RNM-02125.We would like to thank five anonymous referees for their comments.

Appendix: Execution of the models and files generated

Downloading the models

The models are available for free downloading as an ArcGIS tool (susceptibility.tbx) on the follow link: "http://www.ugr.es/local/ren03366/susc_model.rar". For availability on this link, the tool has been compressed by mean of standard compression software: WinRAR, version 3.62.00. It is strongly recommended that this software be used to decompress the tool.

The tool box "susceptibility.tbx", contains two models: the "susceptibility_model" to assess susceptibility, and the "validation_model" to validate the landslide-susceptibility

map. The models are also available in Python, Jscript and VBscript programming languages. The tool susceptibility.tbx has been tested with ArcGIS 9.0, 9.1 and 9.2, running on a WindowsXP operating system. The other tips for using the tool are on the readme_help.pdf file.

Executing (running) the models

The user begins to execute the models by double-clicking on the icons, after introducing the input data and establishing the general parameters (see also the "help" section in the model by right clicking and then clicking on help). The landslide-susceptibility model (susceptibility_model) generates one output datum: the landslide-susceptibility map (suscep_matrix.shp), from three input data: DEM, lithological complexes and landslide inventory. The validation model (validation_model) generates one output datum (the table "adjust.dbf"), from two input data: the landslide-susceptibility map previously obtained (suscep_matrix.shp), and a landslide inventory, which may also be different from the one used in the susceptibility analysis. The model is easily edited (right click and edit the model) and adaptable to the user's needs (i.e. adding more determinant factors). In this case, the way of executing the model is, therefore, to edit the model and execute from the "edit" window, in order to appreciate the steps in which the model shows the user's modifications. The most common changes introduced in the model refer to determinant factors such as vegetation maps, rainfall information, land-use maps, etc., which may be added by the "intersect" tool. Also, different reclassifications may be necessary for particular treatments of some determinant factors; for that purpose simply double click the tool "reclassify" and select some of the available methods (natural breaks, standard deviation, equal intervals or a user-defined method). The most common reclassification is the drawing of the altitude map, since altitude can vary markedly from one area to another, and therefore this possibility is facilitated from the input interface. For the rest of the reclassifications, it is necessary to edit the model.

Determinant factors derived from the DEM

The elevation map ("altitude_7sd.shp") shows a simple reclassification into 7 classes of DEM data, which is a continuous raster surface, converted into a discreet surface ("altitude_7") and finally into a vectorial format ("altitude_7s.shp"). The DEM reclassification is an input datum. This is generalized by classes ("altitude_7sd.shp") in order to simplify the map attributes. The slope-angle layer ("slope_5sd.shp") shows the distribution of slope angles calculated directly by ArcGIS from the DEM. It uses an algorithm of a partial derivate of X (difference of elevation and distance in direction E–W) and the partial derivate of Y (difference of elevation and distance in direction N–S) in a network of 3 × 3 m around each DEM cell ("slope (2)"). Once calculated, the derivates are combined to determine the slope angles which are reclassified ("slope_5"), transformed into a vectorial format ("slope_5s.shp") and generalized. ("slope_5sd.shp"). The slope aspect layer ("aspect_5sd.shp"), accounting for the distribution of this factor, is calculated as the slope angle, from the X and Y partial derivates in a 3 × 3 m network around each of the DEM cells ("aspect (2)"). This continuous map of aspect is reclassified ("aspect_5"), transformed into vectorial ("aspect_5s.shp") and generalized ("aspect_5sd.shp").

Landslide-susceptibility map

Using ArcGIS 9.0 and 9.1, in the landslide-susceptibility map (suscep_matrix.shp) the "crossed_1" column corresponds to the area not affected by the source areas of the landslides for a given combination of factors. The "crossed_2" column shows the area affected by the source areas of the landslides for this combination of classes of determinant factors, and the "crossed_3" column represents the total area of the combination of factors considered. Finally, in the "crossed_po" column the percentage of area affected by the source areas of the landslides in that factor combination is preserved, this being the corresponding susceptibility value.

Using ArcGIS 9.2, in the landslide-susceptibility map (suscep_matrix.shp) the "crossed_VA" column is the area not affected by the source areas of the landslides, the "crossed_1" column shows the area affected by the source areas of the landslides, the "crossed_2" column represents the total area of the combination of factors considered and the "crossed_po" column is the percentage of area affected by the source areas of the landslides.

Validation of the susceptibility map

Using ArcGIS 9.2, in the landslide-susceptibility validation (adjust.dbf) the "adjust" column corresponds to the degree of fit at each susceptibility level. This column (adjust) corresponds to the column "validati_6" if the user is working with either ArcGIS 9.0 or 9.1.

The susceptibility levels are shown in ascending order, so that "OID = 0" in table "adjust.dbf" corresponds to the lowest susceptibility level, in this case very low susceptibility. In ArcGIS 9.0, the model must be executed from the edition window. For the completion of the model, the last tool "calculate field (5)" must be executed individually after previously executing the model, since the last tool does not recognize the new columns that are added until these are generated. This step need not be taken with ArcGIS 9.2, where the model is executed directly.

References

Agterberg FP, Bonham-Carter GF, Wright DF (1989) Weights of evidence modelling: a new approach to mapping mineral potential. In: Agterberg FP, Bonham-Carter GF (eds) Statistical applications in the earth sciences. Geol Surv Can 89(9):171–183

Agterberg FP, Bonham-Carter GF, Cheng Q, Wright DF (1993) Weights of evidence modelling and weighted logistic regression for mineral potential mapping. In: Davis JC, Herzfeld UC (eds) Computer in geology, 25 years of progress. Oxford University Press, Oxford, pp 13–32

Aleotti P, Chowdhury R (1999) Landslide hazard assessment: summary review and new perspectives. Bull Eng Geol Environ 58:21–44. doi:10.1007/s100640050066

ArcGIS (2004) ESRI® ArcMapTM 9.0 License Type: ArcInfo. ESRI Inc.

Ayalew L, Yamagishi H (2005) The application of GIS-based logistic regression for landslide susceptibility mapping in the Kakuda-Yahiko Mountains, Central Japan. Geomorphology 65:15–31. doi:10.1016/j.geomorph.2004.06.010

Bonham-Carter GF (1994) Geographic Information Systems for Geoscientists: modelling with GIS. Pergamon, Ottawa

Bonham-Carter GF, Agterberg FP, Wright DF (1988) Integration of geological datasets for gold exploration in Nova Scotia. Photogramm Eng Remote Sens 54:1585–1592

Brabb EE, Pampeyan EH, Bonilla MG (1972) Landslide susceptibility in San Mateo Country, California. U.S. Geological Survey, Field Studies Map MF-360, scale 1:62500

Canuti P, Casagli N (1996) Considerazioni sulla valutazione del rischio dei frana. Estratto da "*Fenomeni Franosi e Centri Abitati*". Atti del Convegno di Bologna del 27 Maggio 1994. CNR-GNDCI-Linea 2 "Previsione e Prevenzione di Eventi Granosi a Grande Rischio". Pubblicazione no. 846

Carrara A (1988) Multivariate models for landslide hazard evaluation. A "black box" approach. Workshop on natural disasters in European Mediterranean Countries, Perugia, pp 205–224

Carrara A, Merenda L (1974) Metodologia per un censimento deggli eventi franoso in Calabria. Geol Aplicata Idrogeologica 9:237–255

Carrara A, Pugliese-Carratelli E, Merenda L (1977) Computer-based data bank and statistical analysis of slope instability phenomena. Zeitschrift für Geomorphologie N.F 21:187–222

Carrara A, Cardinali M, Detti R, Guzzetti F, Pasqui V, Reichenbach P (1991) GIS techniques and statistical models in evaluating landslide hazard. Earth Surf Process Landf 16:427–445. doi:10.1002/esp.3290160505

Carrara A, Cardinali M, Guzzetti F (1992) Uncertainty in assessing landslide hazard risk. ITC J 1992: 172–183

Carrara A, Cardinali M, Guzzetti F, Reichenbach P (1995) GIS technology in mapping landslide hazard. In: Carrara A, Guzzetti F (eds) Geographical Information Systems in assessing natural hazards. Kluwer Academic Publisher, Dordrecht, pp 135–175

Chacón J, Irigaray C, El Hamdouni R, Fernández T (1996) Consideraciones sobre los riesgos derivados de los movimientos del terreno, su variada naturaleza y las dificultades de evaluación. In: Chacón J, Irigaray C (eds) 6th Congreso Nacional y Conferencia Internacional de Geología Ambiental y Ordenación del Territorio; Riesgos Naturales, Ordenación del Territorio y Medio Ambiente, Granada, pp 407–418

Chacón J, Irigaray C, Fernández T, El Hamdouni R (2002) Susceptibilidad a los movimientos de ladera en el sector central de la Cordillera Bética. In: Ayala-Carcedo FJ, Corominas J (eds) Mapas de Susceptibilidad a los Movimientos de Ladera con Técnicas SIG. Fundamentos y Aplicaciones en España. IGME, Madrid, pp 83–96

Chacón J, Irigaray C, Fernández T, El Hamdouni R (2006) Engineering geology maps: landslides and Geographical Information Systems (GIS). Bull Eng Geol Environ 65:341–411. doi:10.1007/s10064-006-0064-z

Chung CF, Fabbri AG (2003) Validation of spatial prediction models for landslide hazard mapping. Nat Hazards 30:451–472. doi:10.1023/B:NHAZ.0000007172.62651.2b

Chung CF, Fabbri AG, Van Westen CJ (1995) Multivariate regression analysis for landslide hazards zonation. In: Carrara A, Guzzetti F (eds) Geographical Information System in assessing natural hazards. Kluwer Academic Publishers, Dordrecht, pp 107–134

Clerici A, Perego S, Tellini C, Vescovi P (2002) A procedure for landslide susceptibility zonation by the conditional analysis method. Geomorphology 48:349–364. doi:10.1016/S0169-555X(02)00079-X

Cross M (1998) Landslide susceptibility mapping using the Matrix Assessment approach: a Derbyshire case study. In: Maund JG, Eddlestonb M (eds) Geohazards in engineering geology. The Geological Society, vol 15. Engineering Geology Special Publications, London, pp 247–261

Crozier MJ (1986) Landslides: causes, consequences and environment. Croom Helm Pub., Surrey Hills, London

Cruden DM, Varnes DJ (1996) Landslides types and processes. In: Turner AK, Schuster RL (eds) Landslides: investigation and mitigation. National Academic Press, Washington, DC, Sp-Rep 247:35–76

Davis JC, Chung C, Ohlmacher G (2006) Two models for evaluating landslide hazards. Comput Geosci 32:1120–1127. doi:10.1016/j.cageo.2006.02.006

DeGraff JV, Romesburg HC (1980) Regional landslide-susceptibility assessment for wildland management: a matrix approach. In: Coates DR, Vitek JD (eds) Thresholds in geomorphology, vol 19. Alien & Unwin, Boston, pp 401–414

El Hamdouni R (2001) Estudio de Movimientos de Ladera en la Cuenca del Río Ízbor mediante un SIG: Contribución al Conocimiento de la Relación entre Tectónica Activa e Inestabilidad de Vertientes. Unpublished PhD Thesis. Department of Civil Engineering. University of Granada, Spain

Ermini L, Catani F, Casagli N (2005) Artificial neural networks applied to landslide susceptibility assessment. Geomorphology 66:327–343. doi:10.1016/j.geomorph.2004.09.025

Fell R (1994) Landslide risk assessment and acceptable risk. Can Geotech J 31:261–272. doi:10.1139/t94-031

Fernández T (2001) Cartografía, Análisis y Modelado de la Susceptibilidad a los Movimientos de Ladera en Macizos Rocosos mediante SIG: Aplicación a Diversos Sectores del Sur de la Provincia de Granada. Unpublished PhD Thesis. Department of Civil Engineering. University of Granada, Spain

Fernández T, Irigaray C, El Hamdouni R, Chacón J (2003) Methodology for landslide susceptibility mapping by means of a GIS. Application to the Contraviesa area (Granada, Spain). Nat Hazards 30:297–308. doi:10.1023/B:NHAZ.0000007092.51910.3f

Fernández T, Irigaray C, El Hamdouni R, Chacón J (2008) Correlation between natural slope angle and rock mass strength rating in the Betic Cordillera, Granada, Spain. Bull Eng Geol Environ 67:153–164. doi: 10.1007/s10064-007-0118-x

Glade T, Anderson MG, Crozier MJ (eds) (2005) Landslide risk assessment. Wiley, Chichester

Gómez-Pugnaire MT, Galindo-Zaldívar J, Rubatto D, González-Lodeiro F, López V, Jabaloy A (2004) A reinterpretation of the Nevado-Filábride and Alpujárride Complexes (Betic Cordillera): field, petrography and U-Pb ages from orthogneisses (western Sierra Nevada, S Spain). Schweiz Miner Petrog 84:303–322

Goodchild MF (1986) Spatial autocorrelation, CATMOG 47. Geo Books, Norwich

Guzzetti F, Cardinali M, Reichenbach P (1996) The influence of structural setting and lithology on landslide type and pattern. Environ Eng Geosci 2:531–555

Guzzetti F, Carrara A, Cardinali M, Reichenbach P (1999) Landslide hazard evaluation: a review of current techniques and their application in a multi-scale study, Central Italy. Geomorphology 31:181–216

Guzzetti F, Reichenbach P, Cardinali M, Galli M, Ardizzone F (2005) Landslide hazard assessment in the Staffora basin, northern Italian Apennines. Geomorphology 72:272–299

Guzzetti F, Reichenbach P, Ardizzone F, Cardinali M, Galli M (2006) Estimating the quality of landslide susceptibility models. Geomorphology 81:166–184

Hammond CJ, Prellwitz RW, Miller SM (1992) Landslides hazard assessment using Monte Carlo simulation. In: Bell DH (ed) Proceedings of 6th international symposium on landslides, Christchurch, New Zealand, Balkema, 2, pp 251–294

Hansen MJ (1984) Landslide hazard analysis. In: Brundsden D, Prior DB (eds) Slope instability. Wiley, Chichester, pp 523–602

ICA (Instituto de cartografía de Andalucía) (1999) Mapa Digital de Andalucía 1:10.000, hoja 1042. Junta de Andalucía, Seville, 1 digital map

Irigaray C (1995) Movimientos de Ladera: Inventario, Análisis y Cartografía de la Susceptibilidad Mediante un Sistema de Información Geográfica. Aplicación a las Zonas de Colmenar (Málaga), Rute (Córdoba) y Montefrío (Granada). Unpublished PhD Thesis. Department of Civil Engineering. University of Granada, Spain

Irigaray C, Fernández T, Chacón J (1996) Metodología de análisis de factores determinantes de movimientos de ladera mediante un SIG. Aplicación al Sector de Rute (Córdoba, España). In: Chacón J, Irigaray C (eds) 6th Congreso Nacional y Conferencia Internacional de Geología Ambiental y Ordenación del Territorio; Riesgos Naturales, Ordenación del Territorio y Medio Ambiente, Granada, pp 55–74

Irigaray C, Fernández T, El Hamdouni R, Chacón J (1999) Verification of landslide susceptibility mapping. A case study. Earth Surf Process Landf 24:537–544

Irigaray C, Lamas F, El Hamdouni R, Fernández T, Chacón J (2000) The importance of the precipitation and the susceptibility of the slopes for the triggering of landslides along the roads. Nat Hazards 21:65–81

Irigaray C, Fernández T, El Hamdouni R, Chacón J (2007) Evaluation and validation of landslide-susceptibility maps obtained by a GIS matrix method: examples from the Betic Cordillera (southern Spain). Nat Hazards 41:61–79

Iovine G, Di Gregorio S, Lupiano V (2003a) Assessing debris-flow susceptibility through cellular automata modelling: an example from the May 1998 disaster at Pizzo d'Alvano (Campania, southern Italy). In: Rickenmann D, Chen CL (eds) Debris-flow hazards mitigation: mechanics, prediction and assessment. Proceedings of 3rd DFHM international conference, Davos, Switzerland, September 2003, vol 1. Millpress Science Publishers, Rotterdam, pp 623–634

Iovine G, Di Gregorio S, Lupiano V (2003b) Debris-flow susceptibility assessment through cellular automata modeling: an example from 15–16 December 1999 disaster at Cervinara and San Martino Valle Caudina (Campania, southern Italy). Nat Hazards Earth Syst Sci 3:457–468

Jiménez-Perálvarez J, Irigaray C, El Hamdouni R, Fernández T, Chacón J (2005) Rasgos geomorfológicos y movimientos de ladera en la cuenca alta del río Guadalfeo, sector Cádiar-Órgiva (Granada). In: Alonso E, Corominas J (eds) VI Simposio Nacional sobre Taludes y Laderas Inestables. Valencia, Spain, pp 891–902

Kienholz H, Bichsel M, Grunder M, Mool P (1983) Kathmandu-Kakani area, Nepal: mountain hazards and slope stability map. Mountain hazards mapping project map 4 (scale 1:10.000). United Nations University, Tokyo

Maharaj RJ (1993) Landslide processes and landslide susceptibility analysis from an upland watershed a case study from St. Andrew, Jamaica, West Indies. Eng Geol 34:53–79

McCoy J (2004) Geoprocessing in ArcGIS. ESRI Press, Redlands
Mulder HFHM, Van Asch, TWJ (1988) A stochastical approach to landslide hazard determination in a forested area. In: Bonnard C (ed) Proceedings of 5th international symposium on landslides, Laussane, Balkema 2, pp 1207–1210
Okimura T, Kawatani T (1986) Mapping of the potential surface-failure sites on Granite Mountain slopes. In: Gardiner J (ed) International geomorphology, part 1. Wiley, New York, pp 121–138
Ortega M, Nieto F, Rodríguez J, López AC (1985) Mineralogía y estratigrafía de los sedimentos neógenos del corredor de la Alpujarra (Cordillera Bética, España). Boletín de la Sociedad Española de Mineralogía 8:307–318
Pack RT, Tarboton DG, Goodwin CN (1998) The SINMAP approach to terrain stability mapping. In: Proceedings of 8th congress of the international association of engineering geology, Vancouver, British Columbia, Canada, pp 1157–1165
Poli S, Sterlacchini S (2007) Landslide representation strategies in susceptibility studies using weights-of-evidence modeling technique. Nat Resour Res 16:121–134
Remondo J, González A, Díaz de Terán JR, Cendrero A, Fabbri A, Cheng CF (2003) Validation of landslide susceptibility maps: examples and applications from a case study in Northern Spain. Nat Hazards 30:437–449
Rodríguez-Ortiz JM, Hinojosa JA, Prieto C (1978) Regional studies on mass movements in Spain. In: Third IAEG international congress. pp 267–277
SIGMA (Sistema de Información Geológico-Minero de Andalucía) (2002) Mapa Geológico Digital MAGNA 1:50000, hoja 1042. Junta de Andalucía, Seville, 1 digital map
Soeters R, Van Westen JC (1996) Slope instability recognition, analysis, and zonation. In: Turner AK, Schuster RL (eds) Landslides: investigation and mitigation. National Academic Press, Washington, DC, Sp-Rep 247:129–177
Stevenson PC (1997) And empirical method for the evaluation of relative landslide risk. Bull Int Assoc Eng Geol 16:69–72
UNESCO (1976) Guide pour la preparation des cartes géotechniques. UNESCO/IAEG, Paris
Van Westen CJ (1993) Application of geographic information systems to landslide hazard zonation. PhD Dissertation, Technical University Delft, ITC-Publication Number 15, ITC, Enschede, The Netherlands
Van Westen CJ (1994) GIS in landslides hazard zonation: a review with examples from the Andes of Colombia. In: Price MF, Heywood DJ (eds) Mountain environments and geographic information systems. Taylor and Francis, London, pp 135–167
Van Westen CJ (2000) The modelling of landslide hazards using GIS. Surv Geophys 21:241–255
Van Westen CJ, Rengers N, Terlien MTJ, Soeters R (1997) Prediction of the occurrence of slope instability phenomena through GIS-based hazard zonation. Geol Rundsch 86:404–414
Varnes DJ (1978) Slope movements types and processes, In: Schuster RL, Kizek RJ (eds) Landslides: analysis and control. National Academy of Sciences, Washington, DC, Special report 176(2):11–33
Varnes DJ (1984) Landslide hazard zonation: a review of principles and practice. Commission on landslides of the IAEG, UNESCO, Paris. Natural Hazards 3

Rank in Category: NATURAL HAZARDS

Journal Ranking

For **2009**, the journal **NATURAL HAZARDS** has an Impact Factor of **1.217**.

This table shows the ranking of this journal in its subject categories based on Impact Factor.

Category Name	Total Journals in Category	Journal Rank in Category	Quartile in Category
GEOSCIENCES, MULTIDISCIPLINARY	155	80	Q3
METEOROLOGY & ATMOSPHERIC SCIENCES	63	39	Q3
WATER RESOURCES	66	30	Q2

Category Box Plot

For **2009**, the journal **NATURAL HAZARDS** has an Impact Factor of **1.217**.

This is a box plot of the subject category or categories to which the journal has been assigned. It provides information about the distribution of journals based on Impact Factor values. It shows median, 25th and 75th percentiles, and the extreme values of the distribution.

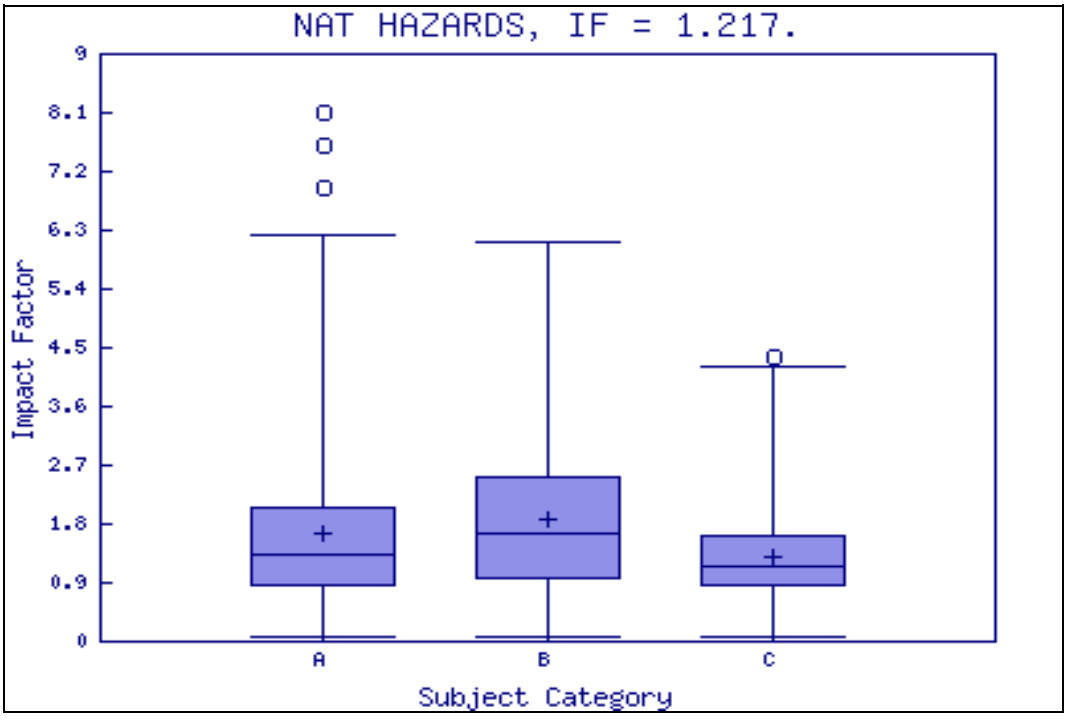

Key

A - GEOSCIENCES, MULTIDISCIPLINARY
B - METEOROLOGY & ATMOSPHERIC SCIENCES
C - WATER RESOURCES

Journal: NATURAL HAZARDS

Mark	Journal Title	ISSN	Total Cites	Impact Factor	5-Year Impact Factor	Immediacy Index	Citable Items	Cited Half-life	Citing Half-life
☐	NAT HAZARDS	0921-030X	1361	1.217	1.577	0.258	128	5.7	9.2

Cited Journal | Citing Journal | Source Data | Journal Self Cites

CITED JOURNAL DATA | CITING JOURNAL DATA | IMPACT FACTOR TREND | RELATED JOURNALS

Journal Information

Full Journal Title: NATURAL HAZARDS
ISO Abbrev. Title: Nat. Hazards
JCR Abbrev. Title: NAT HAZARDS
ISSN: 0921-030X
Issues/Year: 12
Language: ENGLISH
Journal Country/Territory: UNITED STATES
Publisher: SPRINGER
Publisher Address: 233 SPRING ST, NEW YORK, NY 10013
Subject Categories: GEOSCIENCES, MULTIDISCIPLINARY
SCOPE NOTE | VIEW JOURNAL SUMMARY LIST | VIEW CATEGORY DATA
METEOROLOGY & ATMOSPHERIC SCIENCES
SCOPE NOTE | VIEW JOURNAL SUMMARY LIST | VIEW CATEGORY DATA
WATER RESOURCES SCOPE NOTE
VIEW JOURNAL SUMMARY LIST | VIEW CATEGORY DATA

***Eigenfactor*® Metrics**
***Eigenfactor*® Score**
0.00461
***Article Influence*® Score**
0.506

Journal Rank in Categories: JOURNAL RANKING

Journal Impact Factor

Cites in 2009 to items published in: 2008 = 87, 2007 = 193, Sum: 280
Number of items published in: 2008 = 108, 2007 = 122, Sum: 230

Calculation: Cites to recent items 280 / Number of recent items 230 = **1.217**

5-Year Journal Impact Factor

Cites in {2009} to items published in:		Number of items published in:	
2008	=87	2008	=108
2007	=193	2007	=122
2006	=118	2006	=68
2005	=157	2005	=63
2004	=134	2004	=76
Sum:	689	Sum:	437

Calculation: Cites to recent items 689 / Number of recent items 437 = **1.577**

Journal Self Cites

The tables show the contribution of the journal's self cites to its impact factor. This information is also represented in the cited journal graph.

Total Cites	1361
Cites to Years Used in Impact Factor Calculation	280
Impact Factor	1.217

Self Cites	130 (9% of 1361)
Self Cites to Years Used in Impact Factor Calculation	38 (13% of 280)
Impact Factor without Self Cites	1.052

Journal Immediacy Index

Cites in 2009 to items published in 2009 = 33
Number of items published in 2009 = 128
Calculation: Cites to current items 33 / Number of current items 128 = **0.258**

Journal Cited Half-Life

The cited half-life for the journal is the median age of its items cited in the current JCR year. Half of the citations to the journal are to items published within the cited half-life.
Cited Half-Life: 5.7 years

Breakdown of the citations ***to the journal*** by the cumulative percent of 2009 cites to items published in the following years:

Cited Year	2009	2008	2007	2006	2005	2004	2003	2002	2001	2000	1999-all
# Cites from 2009	33	87	193	118	157	134	186	56	61	69	267
Cumulative %	2.42	8.82	23.00	31.67	43.20	53.05	66.72	70.83	75.31	80.38	100

Cited Half-Life Calculations:
The cited half-life calculation finds the number of publication years from the current JCR year that account for 50% of citations received by the journal. Read help for more information on the calculation.

Cited Journal Graph

Click here for Cited Journal data table

This graph shows the distribution by cited year of citations to items published in the journal NAT HAZARDS.
Citations to the journal (per cited year)

- The white/grey division indicates the cited half-life (if < 10.0). Half of the journal's cited items were published more recently than the cited half-life.

- The top (gold) portion

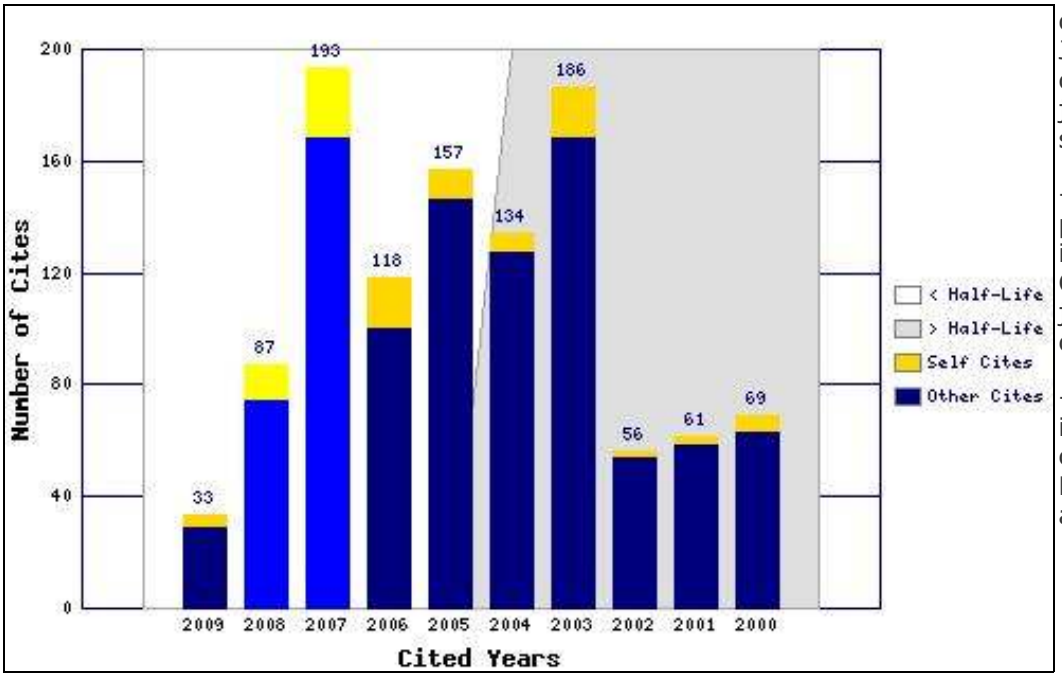

of each column indicates Journal Self Citations: citations to items in the journal from items in the same journal.

- The bottom (blue) portion of each column indicates Non-Self Citations: citations to the journal from items in other journals.

- The two lighter columns indicate citations used to calculate the Impact Factor (always the 2nd and 3rd columns).

Journal Citing Half-Life

The citing half-life for the journal is the median age of the items the journal cited in the current JCR year. Half of the citations in the journal are to items published within the citing half-life.

Citing Half-Life: 9.2 years

Breakdown of the citations ***from the journal*** by the cumulative percent of 2009 cites to items published in the following years:

Cited Year	2009	2008	2007	2006	2005	2004	2003	2002	2001	2000	1999-all
# Cites from 2009	14	145	301	353	332	306	260	207	180	204	1991
Cumulative %	0.33	3.70	10.72	18.94	26.67	33.80	39.86	44.68	48.87	53.62	100

Citing Half-Life Calculations:
The citing half-life calculation finds the number of publication years from the current JCR year that account for 50% of citations in the journal. Read help for more information on the calculation.

Citing Journal Graph

Click here for Citing Journal data table

This graph shows the distribution by cited year of citations from current-year items in the journal NAT HAZARDS.

Citations from the journal (per cited year)

- The white/grey division indicates the citing half-life (if < 10.0). Half of the citations from the journal's current items are to items published more recently than the citing half-life.

- The top (gold) portion of each column indicates Journal Self-Citations: citations from items in the journal to items in the same journal.

- The bottom (blue) portion of each column indicates Non-Self Citations: citations from the journal to items in

other journals.

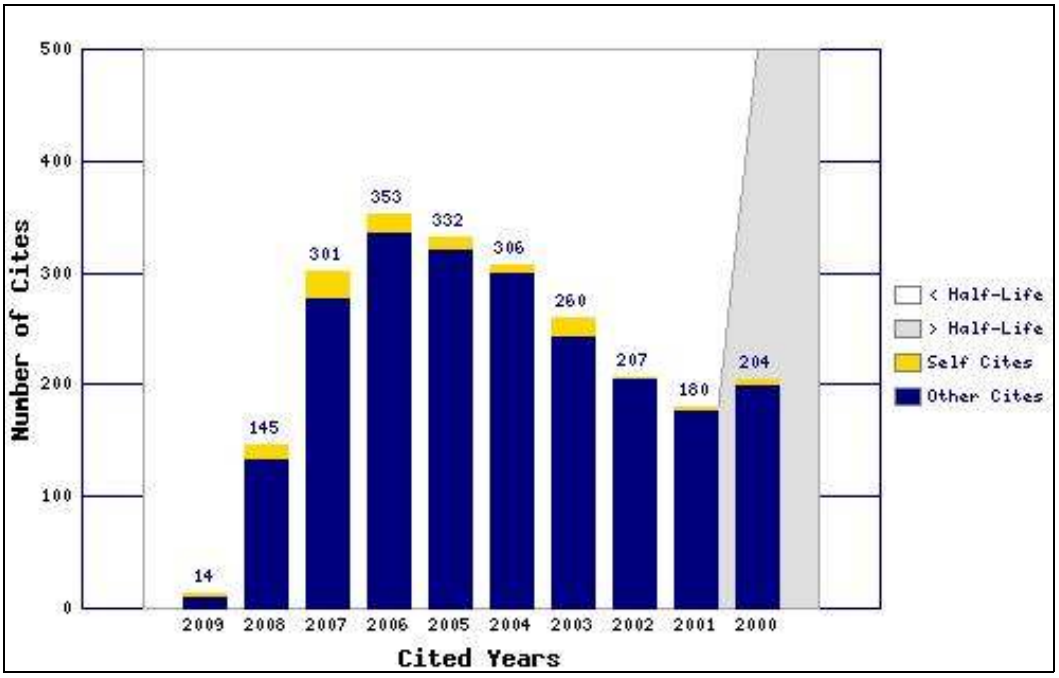

Journal Source Data

	Citable items			
	Articles	**Reviews**	**Combined**	**Other items**
Number in JCR year 2009 (A)	127	1	128	8
Number of references (B)	4099	115	4214	79.00
Ratio (B/A)	32.3	115.0	32.9	9.9

Bull Eng Geol Environ (2011) 70:265–277
DOI 10.1007/s10064-010-0332-9

ORIGINAL PAPER

Landslide-susceptibility mapping in a semi-arid mountain environment: an example from the southern slopes of Sierra Nevada (Granada, Spain)

J. D. Jiménez-Perálvarez · C. Irigaray · R. El Hamdouni · J. Chacón

Received: 28 July 2009 / Accepted: 12 August 2010 / Published online: 2 October 2010

Abstract Landslide susceptibility is analysed in a semi-arid mountain environment, on the southern slope of Sierra Nevada. In a study area of 460 km^2, 252 landslides were inventoried, affecting 3.2% of the total surface area. These landslides were mainly slides and flows on phyllite, schist and marble units in the Inner Zone of the Betic Cordillera. The most relevant determining factors proved to be elevation, slope angle, slope aspect and lithology. Triggering factors include mainly short-term landslide generation during heavy rainfall, as well as sporadic earthquakes or long-term activation by land-use changes, river overexcavation, etc. Although landslide susceptibility, assessed by the GIS matrix method, is predominantly low, some 15% of the study area shows moderate to very high susceptibility, coinciding with the sites of public works in the region. The map drawn was validated by the degree-of-fit method, registering values above 83.2% for the zones of high and very high susceptibility.

Keywords Landslide susceptibility · Bivariate statistical analysis · Semi-arid mountain environment · Sierra Nevada

J. D. Jiménez-Perálvarez (✉) · C. Irigaray · R. El Hamdouni · J. Chacón
Department of Civil Engineering, ETSICCP, University of Granada, Spain, Campus Fuentenueva s/n, Granada 18071, Spain
e-mail: jorgejp@ugr.es
URL: http://www.ugr.es/local/cgl03332

C. Irigaray
e-mail: clemente@ugr.es

R. El Hamdouni
e-mail: rachidej@ugr.es

J. Chacón
e-mail: jchacon@ugr.es

Résumé La sensibilité aux glissements est analysée dans un environnement montagneux semi-aride, sur les versants sud de la Sierra Nevada. Sur un secteur d'étude de 460 km^2, 252 glissements de terrain ont été répertoriés, affectant 3,2% de la surface totale du secteur étudié. Ces glissements de terrain étaient principalement des glissements et des coulées au sein d'unités de phyllites, de schistes et de marbres dans la zone interne de la cordillère bétique. Les facteurs de prédisposition les plus significatifs étaient l'altitude, la pente topographique, la morphologie des pentes et la lithologie. Les facteurs de déclenchement comportaient, pour la génération à court terme de glissements, les fortes pluies ainsi que des séismes sporadiques et, pour les générations sur le long terme, les modifications dans l'usage du sol, le surcreusement des rivières, etc. Bien que la sensibilité aux glissements, évaluée par une méthode matricielle basée sur un système SIG, soit principalement faible, environ 15% du secteur d'étude présente une sensibilité modérée à très forte, coïncidant avec les zones de travaux publics dans la région. La carte dessinée a été validée par une méthode de degré d'ajustement, enregistrant des valeurs supérieures à 83,2% pour les zones de forte à très forte sensibilité.

Mots clés Sensibilité aux glissements · Analyse statistique bivariée · Environnement montagneux semi-aride · Sierra Nevada

Introduction

Landslides (slope movements) can be a natural or man-induced phenomena that generate risks (Varnes 1984; Fell 1994; Glade et al. 2005; Chacón et al. 2006), and therefore it becomes necessary to consider such processes

in land-use planning. Previous research on slope instability in the study zone has described widespread natural gravitational and seismically triggered processes in a semi-arid mountain environment (Thornes and Alcántara-Ayala 1998; Alcántara-Ayala 1999a, b, 2000; El Hamdouni 2001; Fernández 2001; Fernández et al. 2003; Irigaray et al. 2007). Extreme changes in slope-morphology during the Quaternary have resulted in the over-excavation of the drainage network, relief rejuvenation and widespread erosive and deforestation processes (El Hamdouni et al. 2008). To date, some 2,000 landslides have been recorded in different sectors of Sierra Nevada, in the Betic Cordillera (Chacón et al. 2003; Jiménez-Perálvarez et al. 2005), reflecting widespread instability processes triggered occasionally by regional catastrophes that include earthquakes, such as the Andalusian earthquake of 1884 and the Lisbon earthquake of 1755 or, more frequently, heavy rains as in 1996–1997 (Thornes and Alcántara-Ayala 1998; Irigaray et al. 2000).

Preventive and palliative measures could reduce landslide-induced losses by 90% at an estimated cost of 10.3% of the potential losses (Ayala et al. 1987). One of the main measures in this area could be the use of landslide-susceptibility maps to assist decision making in land-use changes or public works planning (Brabb et al. 1972; Chacón et al. 2006). For this purpose, methods involving GIS landslide-susceptibility mapping have been developed over time, with significant contributions from (inter al) Crozier 1986; Carrara et al. 1991; Chung et al. 1995; Canuti and Casagli 1996; Guzzetti et al. 1996, 2005; Soeters and Van Westen 1996; Van Westen et al. 1997; Aleotti and Chowdhury 1999; Irigaray et al. 1999, 2007; Chacón et al. 2006.

This study was undertaken to optimise landslide-susceptibility mapping using a GIS Matrix Method (Irigaray 1995; Cross 1998; Irigaray et al. 1999, 2007; Jiménez-Perálvarez et al. 2009) which had been developed from the approach put forward by DeGraff and Romesburg (1980). The work included an assessment of the GIS Matrix Method (GMM) for determining the influence of local landslide factors in a semi-arid mountain environment (Fernández et al. 2008), landslide-triggering factors (Irigaray et al. 2000) and internal and external validations of the landslide-susceptibility mapping method (Irigaray et al. 1999, 2007; El Hamdouni 2001; Fernández 2001). Some of the main roads and highways of the region are located in the study area, as well as the Rules dam (the only large water reservoir in the Mediterranean part of Granada province); this increases the value of the research, given that the landslide hazard affects different economical activities in the region (intensive agriculture, livestock and tourism).

Climate, geography and geology of the study zone

The study zone (Fig. 1a) is located on the southern slopes of Sierra Nevada (Betic Cordillera) and occupies roughly 460 km^2. The zone is limited to the sub-basin that provides water to the Rules dam and excludes both the north-western sub-basin of the Ízbor River (El Hamdouni 2001) and the southern sub-basin flowing to the Mediterranean Sea (Fernández 2001). The highest summit along the crest of Sierra Nevada (3,492 m) is on the northern edge of the study zone.

The rainfall season spans October to April, whereas from May to September there is a drought period, particularly in July and August, when the average registered precipitation is below 10 mm/month. The temperatures are cold in winter (~8°C) and hot in summer (~23°C), with an elevation effect from a warm coastal border to the much colder summit of the northern Sierra Nevada (Table 1).

Lang's moisture factor (annual precipitation in mm/annual average temperature in °C; Fig. 1b, c) averages 42, corresponding to a semi-arid climate where rainfall is slightly lower than the evapotranspiration (Lang 1915; Köppen 1936). Also the Aridity Index (De Martonne 1942; Botzan et al. 1998) varies between 18, for the warmest months, and 21 for the annual average temperature (Fig. 1d). These values correspond to a semi-arid climate for the warmer months and the boundary between semi-arid and sub-humid for the annual average temperature. Ruiz Sinoga and Martinez Murillo (2009) proposed a similar transitional condition, between semi-arid and sub-humid for a small catchment very close to the study area, with a value of the Aridity Index of 19.7.

The slope morphology alternates between smooth and abrupt relief with over-excavated river channels, showing normal to *rambla* profiles and widespread landslides of variable size and typology. The Quaternary geomorphological evolution shows observable relationships with active tectonic processes (Keller et al. 1996) influencing slope instability conditions and long-term landslide incidence (Thornes and Alcántara-Ayala 1998; Alcántara-Ayala 1999a; El Hamdouni 2001; Jiménez-Perálvarez et al. 2005; El Hamdouni et al. 2008). Hydrology, topography and lithology (including soil cover and vegetation) together with human activity result in a high rate of erosion with regional socio-economic consequences (Castillo et al. 1996).

The study zone (Fig. 1e) is in the Inner Zone of the Betic Cordillera (Balanyá and García-Dueñas 1987), which is formed of metamorphic rocks from both the Nevado-Filabride (Egeler 1964) and Alpujarride Complexes (Van Bemmelen 1927) a well as post-tectonic deposits of Neogene and Quaternary age. In the Nevado-Filabride Complex dark schist and feldspar-bearing micaschist are

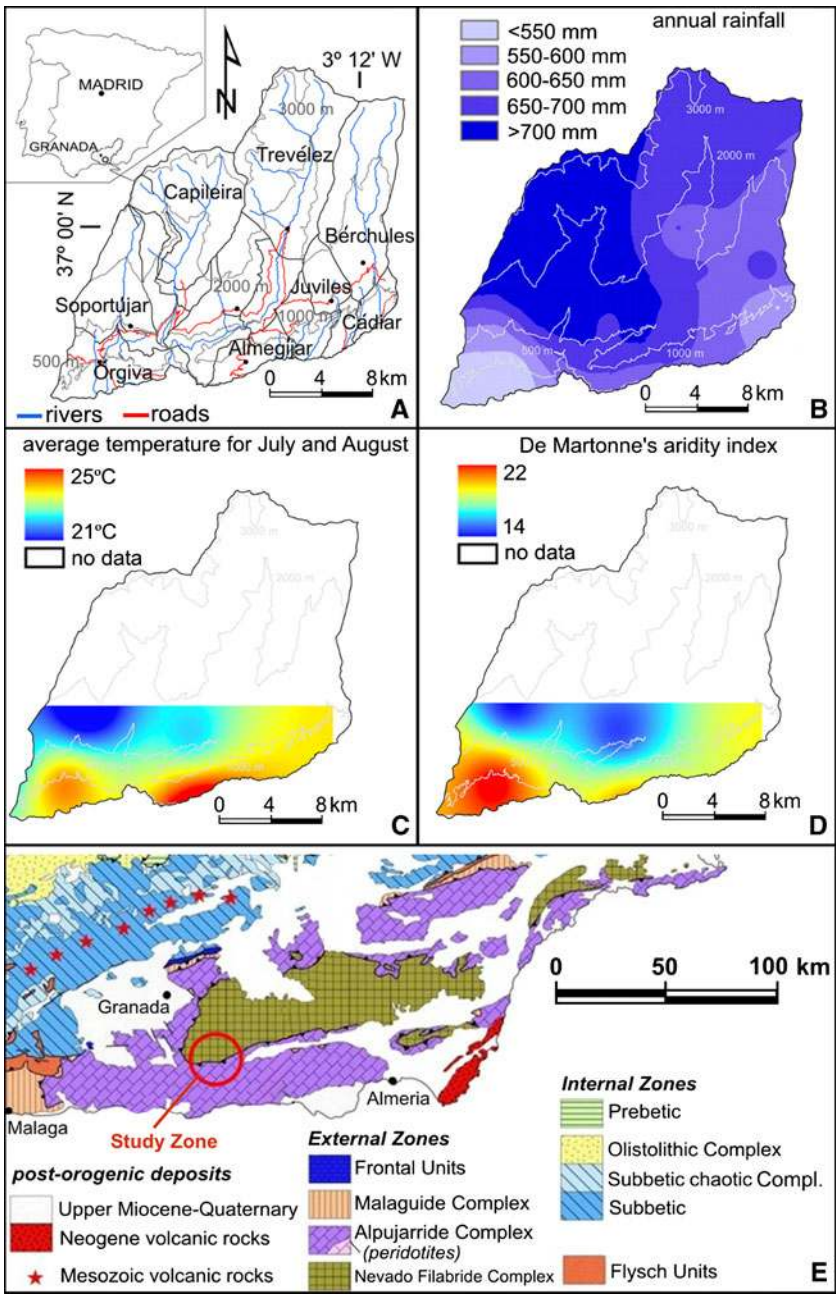

Fig. 1 Geographical (**a**) and geological (**e**) setting of the study zone. **b** Average annual rainfall. **c** Average temperature in July and August. **d** De Martonne's aridity index = annual rainfall in mm/(temperature in °C + 10)

widespread whilst the Alpujárride Complex comprises Triassic calcareous schist, marble, phyllite and quartzite (Gómez-Pugnaire et al. 2004). The Neogene materials are composed of marl and silt covered by conglomerates (Ortega et al. 1985).

Method

The first essential step in this landslide-susceptibility assessment is an accurate identification of unstable slopes and an exhaustive landslide inventory based on aerial photography and conventional field geology surveying including the slope-rupture zone and the downward zone of mass accumulation. The factors describing the current slope conditions are selected from both field observations and GIS cross-analysis of thematic maps.

The initial survey was made using 1:20,000 aerial photos from 1995 supplied by the regional mapping office of the Government of Andalusia in order to delineate the most prominent geomorphological features such as scarps, landslide masses and related features. The field observations were plotted on a 1:10,000 topographical map and included data on lithology, geotechnical features of the soil and rock massif, landslide morphology, type, activity, degree of development, aspect of scarp, mass, vegetation,

Table 1 Average annual temperature and monthly rainfall in different areas of the study zone

Village:	Cádiar		Lanjarón		Órgiva		Pórtugos		Soportújar		Torvizcón	
Month	*T* (°C)	pp (mm)	*T* (°C)	pp (mm)	*T* (°C)	pp (mm)	*T* (°C)	pp (mm)	*T* (°C)	pp (mm)	*T* (°C)	pp (mm)
January	7.2	77.1	8.7	60.2	9.3	70.1	4.7	103.5	6.3	91.5	7.3	71.5
February	8.3	65.2	9.2	55.4	10.5	54.8	6.1	101.1	7.3	83.3	8.5	61.6
March	10.5	53.8	10.6	53.4	12.0	43.2	8.2	77.5	8.5	79.6	11.1	50.8
April	12.6	56.3	12.3	52.0	14.0	44.2	10.4	70.6	10.3	78.1	13.3	48.1
May	16.3	39.2	15.5	34.2	17.8	30.2	14.3	45.6	13.8	43.4	16.7	33.9
June	20.2	15.9	18.8	12.8	20.9	10.9	18.7	20.2	17.1	22.7	21.7	16.5
July	23.9	3.0	22.1	2.7	24.3	2.0	22.8	3.0	21.5	1.8	25.7	3.4
August	24.1	4.4	22.5	4.8	24.5	2.6	22.9	5.1	21.9	7.7	25.4	3.9
September	20.9	27.1	19.9	21.9	21.8	20.2	19.4	26.0	18.9	32.4	22.0	21.7
October	15.5	66.8	15.8	54.3	17.0	56.6	13.3	81.6	13.7	78.9	16.1	60.3
November	10.8	82.5	11.6	68.3	12.9	71.4	8.4	98.7	9.6	94.3	11.4	82.6
December	7.8	88.6	9.5	74.3	10.0	76.7	5.0	112.6	7.0	113.5	7.7	89.0
AAT (°C)	14.8		14.7		16.3		12.8		13.0		15.6	
AR (mm)	580.0		494.4		482.8		745.5		727.1		543.4	

AAT average annual temperature, *AR* annual rainfall

etc. The mapped information was digitalised and introduced into a GIS, with a 1:10,000 orthophoto from 2002 supplied by the Cartographic Institute of Andalusia which shows a pixel size of 0.5 × 0.5 m. (Table 2).

This susceptibility analysis undertaken was based on the following assumptions (Aleotti and Chowdhury 1999): (1) landslides will always occur under the same geological, geomorphological, hydrogeological and climatic conditions as in the past; (2) the primary conditions that cause the landsliding are controlled by identifiable physical factors; (3) the degree of susceptibility can be evaluated; and (4) all types of slope failures can be identified and classified (Concha-Dimas et al. 2007). Under these assumptions, the use of an objective, reproducible and quantitative analysis, such as a bivariate analysis, enables the objective identification of sites with landslide potential (Van Westen 2000). The bivariate statistical analysis undertaken was based on cross analysis of maps of the determining factors for and spatial frequency of slope movements. Whilst it allows an evaluation of the potential relative instability in a broad region by using a series of measurable factors, it is not capable of predicting the susceptibility to slope movements in terms of absolute probability.

Table 2 Scale of data in the sequence of methodological steps

Step	Scale
First geological study area surveying	1:25,000
Landslide inventory	
Remote sensing and aerial photography	1:20,000
Field landslide surveying	1:10,000
GIS digitalization of landslide inventory	1:10,000
Landslide susceptibility assessment: analysis and mapping	1:10,000
Validation of the landslide susceptibility mapping	1:10,000

Slope movements

A database with 252 landslides classified following Varnes's (1978) system (Figs. 2, 3) was prepared. The inventoried landslides (including both rupture and accumulation zones) affect 3.22% of the total study area; 108 slides, 80 flows,

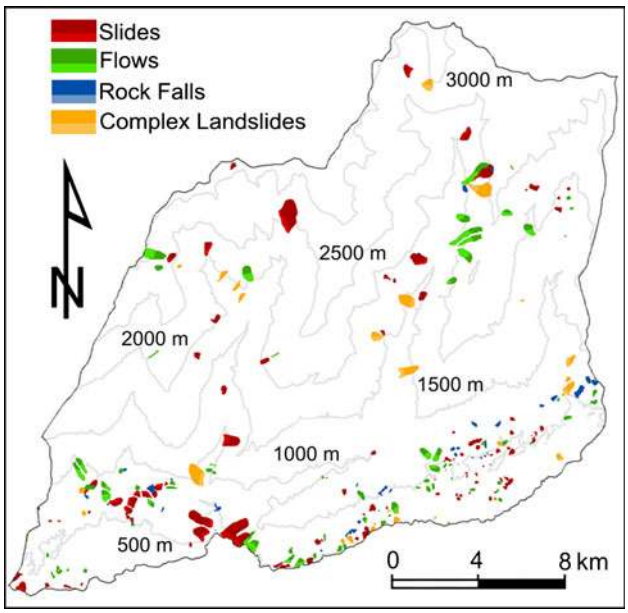

Fig. 2 Landslide-inventory map. In dark the rupture zone (source area) selected for the susceptibility analysis

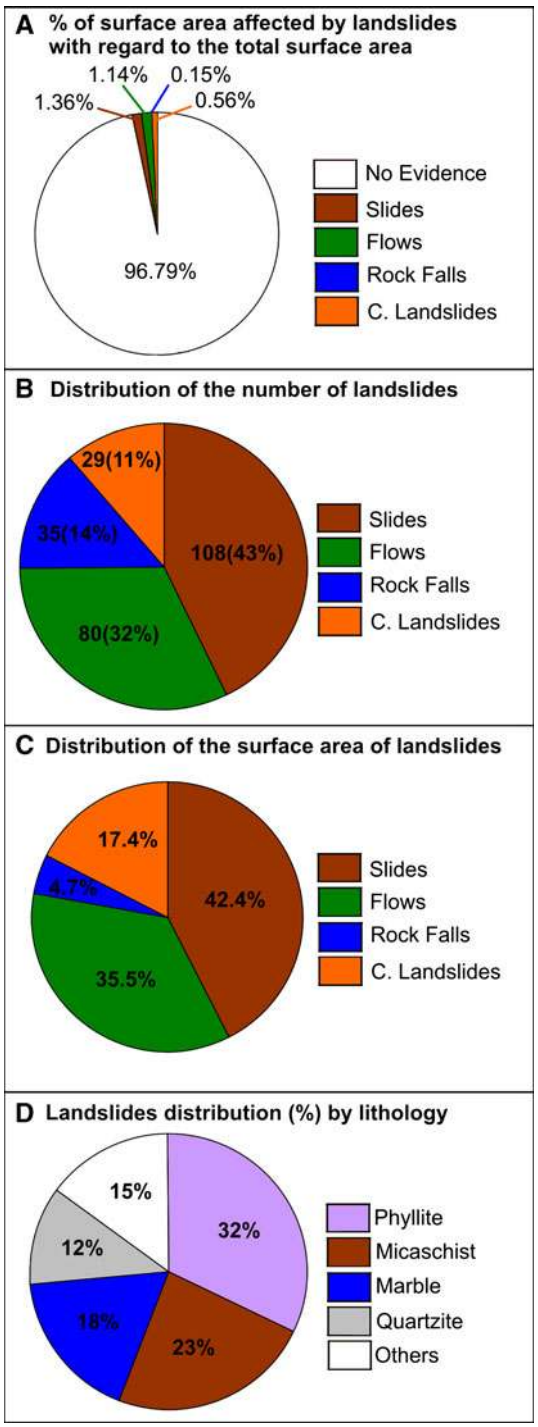

Fig. 3 Landslide distribution in the study zone. **a** Percentage of surface area affected by landslides with regard to the total surface area of the study zone. **b** Number of mapped landslides and percentages by types, with regard to the total landslide inventory. **c** Percentage of mobilised surface area, by types, with regard to the total mobilised surface area. **d** Percentage of mobilised surface area, by lithology, with regard to the total mobilised surface area

35 rock falls and 29 complex landslides were distinguished. Phyllite is the most susceptible lithology, followed by mica schist, marble and quartzite (Tables 3, 4).

Slides

The 108 slides recorded (Fig. 4) were distinguished, representing 43% of the inventoried landslides and affecting 1.36% of the total surface area of the study zone. They are mainly shallow slides with mass thicknesses of <10 m.

From their fresh appearance and preservation of the scarp and mass features, 83% of the slides can be considered recent (UNESCO-WP/WLI 1993). Most had been triggered by the last heavy rain event in the winter/spring of 1996/1997 (Irigaray et al. 2000) although from their morphological appearance some may have been up to 25 years old. Although to some extent obscured by vegetation, it was considered up to 9% may have been up to 50 years old and 8% older. Based on UNESCO-WP/WLI (1993), 20% were at an early and 54% an initial stage of development with 20% showing evidence of an advanced stage of development and 1% being defined as exhausted. Little information is available as to the length of activity, but from local knowledge it is likely to have been for short periods of days or a week, consistent with the findings of Fernández et al. (2009).

Flows

A total of 80 flows were mapped, representing some 32% of the landslide inventory and affecting 1.14% of the total surface area of the study zone. They were generally 3–7 m thick and 45 had small accumulation fans with surface areas of less than 2 ha (Fig. 5). The flows frequently developed on weathered phyllite and micaschist; where their pathways coalesced and/or they accumulated in fans that were mapped as a single landslide. Most of the identified flows which had been partially erased by erosive processes were triggered by 1996/1997 heavy rain event (Irigaray et al. 2000; Chacón et al. 2003).

Rock falls

A total of 35 rock falls were recorded, including small scarps and accumulations of fallen blocks and clasts. They affect only 0.15% of the total surface area and were generally related to marble outcrops and coarse schist layers.

Complex landslides

The 29 complex landslides recorded (11% of the total inventory) affect 0.56% of the study zone. These deep landslides (Alcántara-Ayala 1999a), up to 100 m thick, occur in different materials with variable strengths.

Table 3 Landslide inventory, extension of landslides

Landslide type	*n*	Affected area (including both rupture and accumulation zones)				
		Max. (ha)	Min. (m^2)	Av. (ha)	Tot. (ha)	% of the study zone
Slide	108	83.8	232	5.41	628.1	1.36
Flow	80	35.5	287	4.53	526.0	1.14
Rock fall[a]	35	11.1	453	1.91	68.7	0.15
Complex landslides	29	46.2	3,547	8.58	257.4	0.56
Total	252	83.8	232	5.56	1,480	3.22

[a] Area affected by block pathways

Table 4 Landslide inventory and lithological units affected by slope ruptures

Landslide type	% of inventoried landslides by lithological unit						
	Cc.	Cgm.	Qtz.	Sch	Phy	Mrb.	Msch.
Slide	7.4	8.3	11.1	0.9	33.3	17.6	21.3
Flow	10.0	1.3	11.3	5.0	46.3	0.0	26.5
Rock fall	5.7	0.0	2.9	14.3	0.0	68.6	8.6
Complex landslide	0.0	0.0	24.1	0.0	27.6	6.9	41.4
Total	7.1	4.0	11.5	4.0	32.1	17.9	23.4

Cc. calcareous schist, *Cgm.* conglomerate, *Qtz.* quartzite, *Sch.* schist, *Phyl.* phyllite, *Mrb.* marble, *Msch.* micaschist

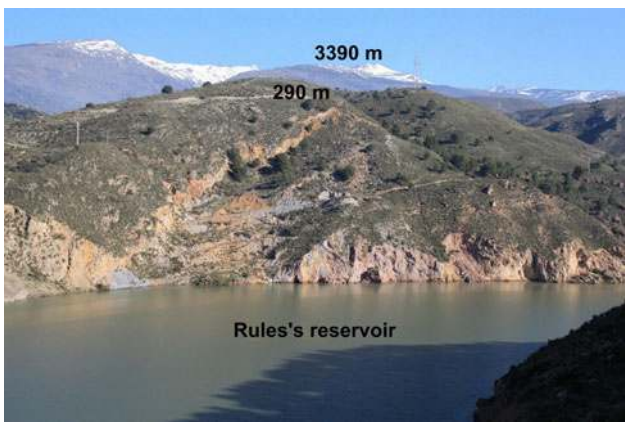

Fig. 4 Planar slide near Carataunas. In the foreground a planar slide of marble on phyllites is shown, in La Cueva creek. In the background some planar slides in phyllites are also visible, on Seco creek channel

Fig. 5 Debris flow over weathered quartzite on the Guadalfeo River right slope, near the villages of Torvizcón and Almegíjar

Determining and triggering factors

Slope-stability conditions depend on a number of physical, geometrical and hydrological conditions, which describe the current stage in the equilibrium profile, as an expression of the geomorphological regional evolution (Thornes and Alcántara-Ayala 1998). The short to fairly long-term evolution of the slope conditions, known as determining factors, may also be described in terms of mechanical properties of the slope materials responsible for a safe balance between disturbing and resisting forces (Hansen 1984). On the other hand, the generation of new landslides is usually associated with more or less short-term or sudden changes in the slope-stability conditions triggered by external or internal forces associated with heavy rains or earthquakes of different magnitudes. These landslide-triggering factors also include human-induced processes such as deforestation, intensive erosion, consequences of some public works, land-use planning, rapid slope excavations, infilling, ore and quarry mining, etc. (Crozier 1984; Hansen 1984).

In areas affected by active tectonics (Keller et al. 1996; El Hamdouni et al. 2008), land uplift and river over-excavation, there is a boundary condition between determining and triggering factors. As the slope equilibrium changes at a higher rate than in regions of passive tectonics, there are long-term/ongoing slope-profile changes. Although shallow landslides are usually triggered by heavy

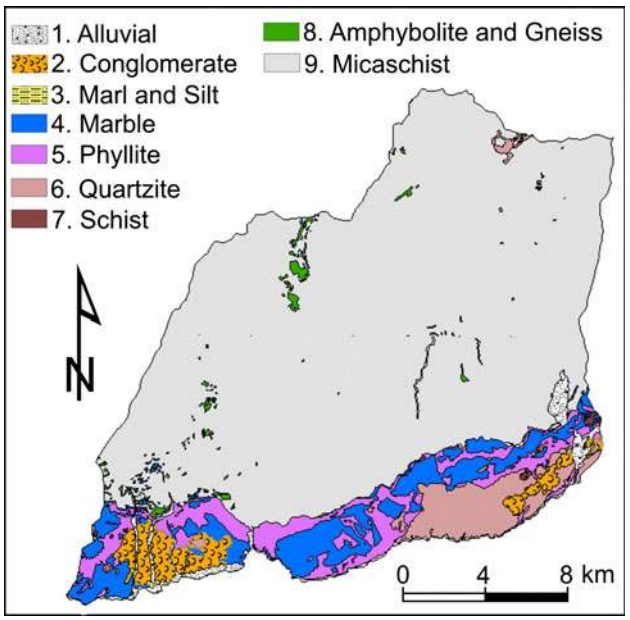

Fig. 6 Map of lithological complexes

rainfall events, deep/old landslides are more likely to be related to long-term slope changes or triggered by strong regional earthquakes (Arango et al. 1995).

As the landslide-susceptibility assessment in this paper is based on determining factors showing clear correlations with the distribution of inventoried landslide ruptures (Chacón et al. 1993, 1994; Irigaray et al. 2007; Fernández et al. 2008), an analysis by crossed tabulation (contingency tables) was performed between the source areas (or rupture zones) and determining factors. A number of different correlation coefficients were calculated and significance tests were used to identify the most influencing factors, i.e. Chi-square, coefficient of linear correlation of the contingency coefficient, Tschuprow's T and Cramer's V coefficients (Table 5). The determining factors showing the highest degree of association with the landslide inventory were lithology, slope angle, slope aspect and altitude (or elevation).

Determining factors derived from DEM

In the GIS approach, the digital terrain models (DTMs) are the main source of data in the description and quantitative analysis of the physical environment (Burrough 1988). The DTMs developed from the DEM comprise the determining factors. The DEM offers information on the z-coordinate (elevation) in any of the (x, y) georeferenced coordinates. The DEM used in this research was derived from the DTM of Andalusia (Junta de Andalucía 2005) generated from 1:20,000 aerial photos and composed of a regular network of 10 × 10 m. A triangular irregular network (TIN) was then applied to transform the vectorial data (points and lines) into a raster format with a pixel size of 10 × 10 m.

Table 5 Correlation between the source areas of the landslides and the determining factors

Factor	χ^2	R	T	V
Altitude	6.27	0.40	0.07	0.12
Illumination	3.51	0.35	0.06	0.09
Lithological contacts	1.20	0.27	0.05	0.05
Vertical curvature	1.12	0.26	0.03	0.05
Faults	0.25	0.18	0.02	0.02
Slope aspect	6.80	0.41	0.09	0.12
Precipitation (annual mean)	2.06	0.31	0.05	0.07
Lithology	12.95	0.48	0.10	0.17
Distance to watercourses	0.32	0.19	0.03	0.03
Land-use	0.46	0.21	0.02	0.03
Slope angle	6.75	0.41	0.09	0.12

χ^2 Chi-square, R lineal and contingency correlation coefficient C, $R = \sqrt{(C/C_{max})}$, T Tschuprow's T, V Cramer's V

Lithology, slope angle, slope aspect and altitude are the determining factors which show the highest degree of association

Elevation This is a useful determining factor previously applied in nearby mountain areas (Fernández et al. 2008). On the southern edge of Sierra Nevada, where the study zone is located, there is a clear connection between the elevation and the tectonic units. The average height over the study area is 1,780 m, with 40% above 2,000 m and 25% above 2,500 m. With a range of elevations between 3,482 and 190 m in a horizontal distance of 20 km, the DEM used a contour interval of 500 m (Table 6a).

Slope angle This is one of the most common determining factors in quantitative landslide-susceptibility analyses from Brabb et al. (1972) to the present (Chacón et al. 2006; Fernández et al. 2008). As shown in Table 6b, five intervals were selected: 0–5° (gentle); 5–15° (fairly steep); 15–25° (steep); 25–35° (very steep); and 35–90° (extremely steep). The very steep slopes (30%) correspond to over-excavated valleys sometimes with tributary rivers, although along the main channel the slope angle is fairly steep to steep whilst the Neogene Órgiva basin has a gentle to fairly steep slope.

Slope aspect This is measured to the magnetic direction, ±45°. As with the elevation factor, this is also only indirectly related to landslides. In order to simplify the analysis, the GIS attitude map was re-classified into the four compass directions and flat (Table 6c). Less than 1% of the land is flat, with the majority (38%) oriented southwards, towards the Mediterranean Sea.

Table 6 Distribution of classes of landslide-susceptibility determining factors in the study area

	Surface area	
	%	km^2
(a) Elevation (m)		
190–500	3.94	18.127
500–1,000	14.65	67.413
1,000–1,500	18.54	85.332
1,500–2,000	21.76	100.16
2,000–2,500	20.55	94.604
2,500–3,000	17.43	80.225
>3,000	3.13	14.427
(b) Slope angle (°)		
0–5	3.52	16.211
5–15	24.54	112.94
15–25	40.73	187.48
25–35	29.50	135.80
>35	1.71	7.854
(c) Slope aspect		
Flat	0.74	3.386
North	4.88	22.46
East	32.32	148.76
South	38.44	176.95
West	23.62	108.73
(d) Lithological unit		
1. Alluvial, calcrete, travertine	2.00	9.199
2. Conglomerate	2.93	13.475
3. Marl and silt	0.02	0.109
4. Marble	7.31	33.649
5. Phyllite	6.12	28.170
6. Quartzite	4.27	19.646
7. Bluish schist	0.11	0.529
8. Amphibolite and gneiss	0.78	3.569
9. Micaschist	76.46	351.94

Factors not related to the DEM

Factors controlling the mechanical behaviour of the slope are also important, especially the lithology. As noted above, the regional setting is related to the alpine crustal collision between the African and Eurasia plates, with large tectonic nappes composed by metamorphic rocks and Neogene sedimentary deposits along faulted corridors (Aldaya et al. 1979). For research purposes, UNESCO (1976) recommended the grouping of soil and rock units into 'lithological complexes' (Fig. 6) with qualitative similarities in shear strength and contribution to the slope stability (Table 6d). The following lithological complexes are distinguished, with an indicative estimation of most frequently measured basic rock mass ratio shown as RMR.

Unit 1: Alluvial colluvial and slope-scree, calcrete and travertine (very limited surface area).
Unit 2: Conglomerate with broadly rounded clasts in a sandy to silty matrix with some cementing. (RMR = 30).
Unit 3: Yellowish marl and silt (limited surface area).
Unit 4: Marble of Upper Palaeozoic to Triassic age with strong intact rock and highly variable discontinuities. Usually on phyllite or calcareous schist units, showing different crushing and degree of metamorphism, the composition varies from calcium to magnesium-bearing carbonates (RMR = 60).
Unit 5: Phyllite. Grey to bluish metamorphic shale interlayered with gypsum or calcareous schist. The outcrops are highly weathered up to one or two meters in depth; the residual materials consist of low plasticity silt or silty sand (RMR = 15).
Unit 6: Quartzite. A resistant remnant in the smoothed landscape of the Sierra de la Contraviesa, alternating with biotitic micaschists that are deeply weathered in superficial outcrops (RMR = 45).
Unit 7: Bluish schist usually below the quartzite units, with variable discontinuities whose relationship with the slope determines the stability (RMR = 25).
Unit 8: Amphibolite and basic gneiss are found in a few outcrops; although their mineralogy differs, their effect on slope stability is similar (RMR = 50).
Unit 9: Micaschist. The most extensive outcrop in the study area, particularly towards the north, it includes dark graphite-bearing and lighter feldspar and epidote-bearing schists. It is usually weathered to a depth of 1 m but below this its strength increases rapidly (RMR = 40).

In the study zone, the most common lithologies are micaschist (Unit 9—76%), marble (Unit 4—7.3%) and phyllite (Unit 5—6.12%).

Susceptibility analysis

The susceptibility approach was designed by the USGS in the 1960s as a qualitative way to prepare landslide maps or to delineate zones affected by landslides, assessing the propensity of a given slope unit to generate a landslide (Brabb et al. 1972). A recent comprehensive review of papers, concepts and methods was presented by Chacón et al. (2006) including previous methods based on Guzzetti et al. (1999), Van Westen (2000), etc.

The susceptibility maps are based on spatial data, in the sense that both the landslide inventory and the selected set of factors determining the stability conditions describe the observed engineering geology of the study zone during the research. Further temporal data such as landslide activity,

landslide diachroneity (chronology), recorded velocities, return period, yearly/monthly/daily rainfall, earthquake records, etc. are necessary for hazard assessment and mapping whilst data on the consequences of the landslides (damaged or damageable elements of the territory and their vulnerability) are necessary to draw landslide-risk maps (Chacón et al. 2006).

A landslide-susceptibility map offers a spatial view of zones with qualitatively similar slope-stability conditions and ability to generate landslides. Given the marked differences between the various types of landslides, for large-scale maps, it is advisable to apply different methods of susceptibility analysis to provide a separate susceptibility assessment for each landslide type. In middle- to small-scale susceptibility maps the method may be comprehensive with respect to the inventory, with a set of determining factors validated for the purpose of drawing the map (Chacón et al. 1993, 1994). The susceptibility map is useful for preparing regional or local land-use planning and the preliminary design of corridors or civil-engineering works, in order to minimise the consequences of developing susceptible land where landslide may add unexpected costs or even result in loss of life.

In this study, the GMM of susceptibility analysis is applied (Irigaray 1995) as the landslide-susceptibility maps can be prepared through a process performed entirely in a GIS application, without the need of external computer packages; it has been validated as a method of analysis by subsequent landslides (Irigaray et al. 1999; 2007; El Hamdouni 2001; Fernández 2001; Fernández et al. 2003). In addition, an application of ArcGIS (ESRI), with Model Builder, is now available for the automatic preparation of landslide-susceptibility maps with GMM (Jiménez-Perálvarez et al. 2009).

The GMM is based on the computation of three matrices: a landslide inventory matrix (LM), a matrix of the total surface of the study area (TSM), and a susceptibility matrix (SM). First, a LM is established by calculating areas or extensions affected by the source areas (i.e. rupture zone) of the landslides in each combination of classes of the selected determining factors; source areas are identified by the shape of the mapped scarps as the first setting of the mass prior to the landslide process. The TSM matrix is calculated by making all the possible combinations among the classes of determining factors selected, and then calculating the area occupied by each combination. Finally, in the SM, each cell shows a value calculated by dividing the value of the cell in the LM by the value of the cell in the TSM. The cell values in the SM represent an assessment of relative susceptibility corresponding to each combination of determining factors in the cell. Each SM value shows the percentage of source areas in each combination of determining factors with regard to the total area occupied by the respective combination of determining factors. The susceptibility maps are based on five levels of classification, automatically assigned to each zone by using the natural-breaks method (Irigaray et al. 2007; ArcGIS 2004). In this method, class breaks are determined statistically by finding adjacent pairs of features which show relatively large differences in data values (ArcGIS 2004).

The values contained in the SM represent the proportion of landslides with regard to the total surface of the study zone, and give a relative susceptibility for each combination of factors. As each pixel of the map, or given point in the study area, is characterized by a given combination of factors, its relative susceptibility is shown in the SM for that particular combination of factors.

Results

For the analysis and definition of susceptibility zones, the aforementioned determining factors with the highest correlation to landslide sources were selected: elevation, slope angle, slope attitude and lithological unit (Table 5). The susceptibility values varied between 0 and 100 in each combination of classes of determinant factors and assigned to five levels: very low (1–2%); low (up to 5%); moderate (up to 10%); high (up to 15%); and very high (>15%); see Fig. 7 and Tables 7 and 8 (Irigaray 1995; El Hamdouni 2001; Fernández et al. 2003, 2008; Irigaray et al. 2007; Jiménez-Perálvarez et al. 2009).

For susceptibility to rock falls, the identification of the source map is limited by the distribution of blocks and the

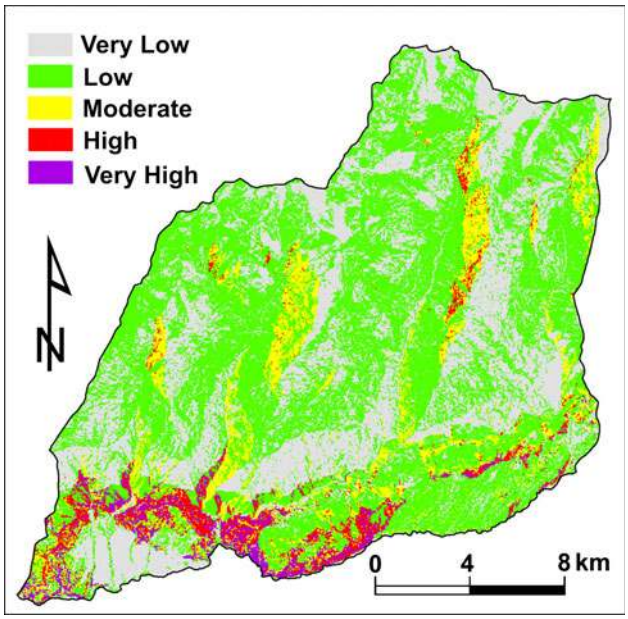

Fig. 7 Map of accumulated landslide susceptibility of the study area

morphology of the scarp, hence different intervals were used (Irigaray et al. 2007; Jiménez-Perálvarez et al. 2009): very low (0); low (1%); moderate (3%); high (5%); and very high susceptibility (8%).

The study area shows a limited incidence of slides, expressed by the 94.3% of the total area calculated as having low to very low susceptibility (Table 7a), concentrated particularly in the north where a weathered mica schist unit is widespread at the highest elevations.

Although only a small surface area falls into the high and very high susceptibility zones concentrated on the southern edge of the study area, particularly where the Neogene conglomerates are over-steepened near the tributaries of the Guadalfeo River. It is of note that the Rules dam, on the Guadalfeo River, is in this zone.

Only 0.7% of the study area (Table 7b) has a high to very high susceptibility to flows. The triggering factors are sudden storms or intense daily rainfall where accumulation deposits are rapidly eroded. In the most affected areas, around the Rules dam, the infrastructures and roads are commonly damaged.

Table 7 Surfaces covered by the landslide-susceptibility zones in the study area

	%	km^2
(a) Slide susceptibility		
Very low	67.91	312.50
Low	26.36	121.31
Moderate	3.79	17.44
High	1.30	5.96
Very high	0.64	2.93
(b) Flow susceptibility		
Very low	72.18	332.14
Low	24.51	112.79
Moderate	2.64	12.14
High	0.39	1.78
Very high	0.28	1.29
(c) Rock-fall susceptibility		
Very low	97.32	447.82
Low	2.59	11.92
Moderate	0.04	0.18
High	0.03	0.14
Very high	0.02	0.10
(d) Complex-landslide susceptibility		
Very low	84.28	387.81
Low	14.92	68.65
Moderate	0.61	2.80
High	0.19	0.87
Very high	0.00	0.00

Only 0.1% of the study area was classified as moderately to highly susceptible to rock falls (Table 7c) and 0.8% of the area as moderately to highly susceptible to complex landslides with 99.2% falling into the low to very low class (Table 7d).

When all the results were combined in the general map, 94% of the study area showed very low, low or moderate landslide susceptibility to accumulated landslides, with only 6% registering high or very high susceptibility (Table 8). These highly susceptible areas (Fig. 7) appear along the banks of the main river and along the boundary between the marble and phyllite units. Again, the Rules dam is highly susceptible.

Internal validation of the susceptibility maps

An internal calibration of the susceptibility maps was made with the same landslide inventory used for the analytical procedure (Guzzetti et al. 2006; Remondo et al. 2003). The quality of the maps was assessed by spatial autocorrelation and the degree of fit between a given set of data and the maps (Goodchild 1986).

The degree of fit (DF), as applied to landslide maps, is defined as follows:

$$\mathrm{DF}_i = \frac{m_i/t_i}{\sum m_i/t_i}$$

where m_i is the area occupied by the source areas of the landslides at each susceptibility level i, and t_i is the total surface area covered by that susceptibility level. The degree of fit for each susceptibility level represents the percentage of mobilised area located in each susceptibility class. The lower the degree of fit (less than 7%) in the low and very low susceptibility classes (relative error), and the higher the degree of fit in the high or very high susceptibility classes (relative accuracy), the higher the quality of the susceptibility map will be (Fernández et al. 2003; Irigaray et al. 2007).

Table 8 Total susceptibility to all landslides considered

Landslide susceptibility	Surface area	
	%	km^2
Very low	32.99	151.81
Low	52.26	240.45
Moderate	8.86	40.77
High	3.60	16.56
Very high	2.29	10.56

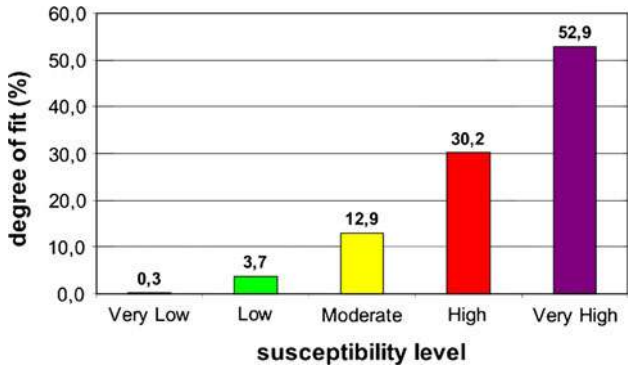

Fig. 8 Distribution of landslides by susceptibility classes

The degree of adjustment (Fig. 8) required for the high and very high susceptibility classes reached 83% whilst for the low and very low classes it was only 4%.

Discussion and conclusions

In the study zone, 3.22% of the surface area is affected by landslides. Planar slides and flows predominate, with a lower proportion of rock falls and complex landslides. The lithological units most susceptible to landslides are phyllites, micaschists and marbles. The landslides are usually shallow, i.e. <10 m depth, although some large, deep complex landslides occur.

The most frequent planar slides are usually larger than the other landslides. Although most of the slides in the study area are dormant, recent data have shown very low velocity activity (<10 mm/year) in the La Serreta planar slide (Fernández et al. 2009).

The observed remnant of debris flows (deposits, pathways, scars etc.) suggest they are usually small and coalescent with other contemporaneous flows. There is only a small incidence of rock falls, which affect only limited areas.

In summary, the results of the landslide-susceptibility mapping using the GMM show a study area with predominantly low susceptibility. Nevertheless, about 15% is moderately to very highly susceptible, with rather more planar slides.

One constraint of the GMM is the need for a previous exhaustive landslide inventory of the study area. In the case of rock slides, or landslides affecting rock massifs and cohesive overconsolidated sediments, the remnants of the slope disruption in the rupture zone, or the accumulated mass, are observable over periods of time, enabling remote sensing and field inventory. This is aided by the thin vegetation and the erosional effect of heavy rainfall almost yearly in these semi-arid regions. However, the evidence of debris flows may be effaced quickly, except when the accumulated mass or the pathway pattern reaches larger dimensions.

Although the time scale over which evidence of landsliding remains visible has not been quantified for each type of landslide, it is considered that most of the landslides of the study area have been inventoried, except perhaps some shallow small features and debris flows which may have been underestimated.

The value of a validated landslide-susceptibility map is that it assists in making a quick and simple assessment of the most appropriate terrains for civil engineering or of building projects, or areas where more detailed studies would be necessary. Nevertheless, it is vital to emphasise the importance of an adequate engineering-geological approach, including field and remote-sensing surveys, in order to compile the basic data for landslide prevention; the inventory of landslides, the thematic layers related to the determining factors, and also all the information available on landslide-triggering factors.

Acknowledgments This research was supported by projects CGL2005-03332 and CGL2008-04854 funded by the Ministry of Science and Education of Spain, and Excellence Project P06-RNM-02125, funded by the Regional Government. Rainfall dates have been supplied by the National Meteorological Institute of Spain. It was developed in the RNM121 Research Group funded by the Andalusian Research Plan.

References

Alcántara-Ayala I (1999a) Modelling deep-seated slope failures in semi-arid southern Spain. Geofís Int 38(1):49–59

Alcántara-Ayala I (1999b) The Torvizcón, Spain, landslide of February 1996: the role of lithology in a semi-arid climate. Geofís Int 38(3):175–184

Alcántara-Ayala I (2000) Índice de susceptibilidad a movimientos del terreno y su aplicación en una región semiárida. Rev Mex Cienc Geol 17(1):66–75

Aldaya F, Martínez-García D, Díaz de Federico A, Puga E, García-Dueñas V, Navarro-Vilá F (1979) Mapa Geológico de España 1:50.000, hoja n° 1042. IGME

Aleotti P, Chowdhury R (1999) Landslide hazard assessment: summary review and new perspectives. Bull Eng Geol Environ 58(1):21–44. doi:10.1007/s100640050066

Arango JR, Blázquez R, Chacón J, López C (1995) Soil liquefaction potential induced by the Andalusian earthquake of 25 December 1884. Nat Hazards 12(1):1–17. doi:10.1007/BF00605278

ArcGIS (2004) ESRI® ArcMap™ 9.0 License Type: ArcInfo. ESRI Inc

Ayala FJ, Elizaga E, González de Vallejo LI (1987) Impacto económico y social de los riesgos geológicos en España. IGME, Madrid, p 134

Balanyá JC, García-Dueñas V (1987) Les directions structurales dans le Domaine d'Alborán de part et d'autre du Détroit de Gibraltar. Comptes Rendus de l'Académie des Sciences de Paris. Serie II 304(15):929–932

Botzan TM, Mariño MA, Necula AI (1998) Modified de Martonne aridity index: application to the Napa Basin, California. Phys Geogr 19(1):55–70

Brabb EE, Pampeyan EH, Bonilla MG (1972) Landslide susceptibility in San Mateo Country, California. U.S. Geological Survey, Field Studies Map MF-360, scale 1:62500

Burrough P (1988) Principles of geographical information systems for land resources assessment. Oxford University Press, London, p 194

Canuti P, Casagli N (1996) Considerazioni sulla valutazione del rischio dei frana. Estratto da "Fenomeni Franosi e Centri Abitati". Atti del Convegno di Bologna del 27 Maggio 1994. CNR-GNDCI-Linea 2 "Previsione e Prevenzione di Eventi Granosi a Grande Rischio". Pubblicazione no. 846

Carrara A, Cardinali M, Detti R, Guzzetti F, Pasqui V, Reichenbach P (1991) GIS techniques and statistical models in evaluating landslide hazard. Earth Surf Process Landf 16(5):427–445. doi:10.1002/esp.3290160505

Castillo A, Martín-Rosales W, Osorio R (1996) Erosión hídrica en la cuenca del río Guadalfeo (Granada); estudio comparativo de las metodologías de la U.S.L.E y Fournier. Geogaceta 19:142–145

Chacón J, Irigaray C, Fernández T (1993) Methodology for large scale landslide hazard mapping in a G.I.S. In: Seventh international conference and field workshop on landslides, vol 1. Bratislava, Eslovaquia, pp 77–82

Chacón J, Irigaray C, Fernández T (1994) Large to middle scale landslides inventory, analysis and mapping with modelling and assessment of derived susceptibility, hazards and risks in a GIS. In: Seventh IAEG international congress, vol 1. Balkema, Rotterdam, pp 4669–4678

Chacón J, Irigaray C, Fernández T, El Hamdouni R (2003) Susceptibilidad a los movimientos de ladera en el sector central de la Cordillera Bética. In: Ayala FJ, Corominas J (eds) Mapas de susceptibilidad a los movimientos de ladera con técnicas SIG. Fundamentos y Aplicaciones en España. IGME, Madrid, pp 83–96

Chacón J, Irigaray C, Fernández T, El Hamdouni R (2006) Engineering geology maps: landslides and geographical information systems (GIS). Bull Eng Geol Environ 65(4):341–411. doi:10.1007/s10064-006-0064-z

Chung CF, Fabbri AG, Van Westen CJ (1995) Multivariate regression analysis for landslide hazards zonation. In: Carrara A, Guzzetti F (eds) Geographical information system in assessing natural hazards. Kluwer Academic Publishers, Dordrecht, pp 107–134

Concha-Dimas A, Campos-Vargas M, López-Miguel C (2007) Comparing heuristic and bivaritate GIS-based methods for refining landslide susceptibility maps and northern Mexico City. Environ Eng Geosci 13(4):277–287. doi:10.2113/gseegeosci.13.4.277

Cross M (1998) Landslide susceptibility mapping using the matrix assessment approach: a Derbyshire case study. In: Maund JG, Eddlestonb M (eds) Geohazards in engineering geology. The Geological Society, vol 15. Engineering Geology Special Publications, London, UK, pp 247–261

Crozier MJ (1984) Field assessment of slope instability. In: Brundsden D, Prior DH (eds) Slope instability. Wiley, New York, pp 103–142

Crozier MJ (1986) Landslides: causes, consequences and environment. Croom Helm Publishers, Surrey Hills, London, p 272

De Martonne E (1942) Nouvelle carte mondiale de l'indice d'aridité. Annales de Geographie 288:241–250

DeGraff JV, Romesburg HC (1980) Regional landslide-susceptibility assessment for wildland management: a matrix approach. In: Coates DR, Vitek JD (eds) Thresholds in geomorphology, vol 19. Alien & Unwin, Boston, pp 401–414

Egeler CG (1964) On the tectonics of the eastern Betic Cordilleras (SE Spain). Int J Earth Sci (Geologische Rundschau) 53(1):260–269. doi:10.1007/BF02040750

El Hamdouni R (2001) Estudio de Movimientos de Ladera en la Cuenca del Río Ízbor mediante un SIG: Contribución al Conocimiento de la Relación entre Tectónica Activa e Inestabilidad de Vertientes. Unpublished PhD Thesis, Department of Civil Engineering, University of Granada, Spain, 429 pp

El Hamdouni R, Irigaray C, Fernández T, Chacón J, Keller EA (2008) Assessment of relative active tectonics, southwest border of the Sierra Nevada (southern Spain). Geomorphology 96(1–2): 150–173. doi:10.1016/j.geomorph.2007.08.004

Fell R (1994) Landslide risk assessment and acceptable risk. Can Geotech J 31(2):261–272. doi:10.1139/t94-031

Fernández T (2001) Cartografía, análisis y modelado de la susceptibilidad a los movimientos de ladera en macizos rocosos mediante SIG: Aplicación a diversos sectores del sur de la provincia de Granada. Unpublished PhD Thesis, Department of Civil Engineering, University of Granada, Spain, 648 pp

Fernández T, Irigaray C, El Hamdouni R, Chacón J (2003) Methodology for landslide susceptibility mapping by means of a GIS. Application to the Contraviesa area (Granada, Spain). Nat Hazards 30(3):297–308. doi:10.1023/B:NHAZ.0000007092.51910.3f

Fernández T, Irigaray C, El Hamdouni R, Chacón J (2008) Correlation between natural slope angle and rock mass strength rating in the Betic Cordillera, Granada, Spain. Bull Eng Geol Environ 67(2):153–164. doi:10.1007/s10064-007-0118-x

Fernández P, Irigaray C, Jiménez-Perálvarez J, El Hamdouni R, Crosetto M, Monserrat O, Chacón J (2009) First delimitation of areas affected by ground deformations in the Guadalfeo River Valley and Granada metropolitan area (Spain) using the DInSAR technique. Eng Geol 105(1–2):84–101. doi:10.1016/j.enggeo.2008.12.005

Glade T, Anderson MG, Crozier MJ (eds) (2005) Landslide risk assessment. Wiley, Chichester, pp 832

Gómez-Pugnaire MT, Galindo-Zaldívar J, Rubatto D, González-Lodeiro F, López V, Jabaloy A (2004) A reinterpretation of the Nevado-Filábride and Alpujárride complexes (Betic Cordillera): field, petrography and U-Pb ages from orthogneisses (western Sierra Nevada, S Spain). Schweiz Miner Petrogr Mitt 84(3): 303–322

Goodchild MF (1986) Spatial autocorrelation, CATMOG 47. Geo Books, Norwich, pp 56

Guzzetti F, Cardinali M, Reichenbach P (1996) The influence of structural setting and lithology on landslide type and pattern. Environ Eng Geosci 2(4):531–555

Guzzetti F, Carrara A, Cardinali M, Reichenbach P (1999) Landslide hazard evaluation: a review of current techniques and their application in a multi-scale study, Central Italy. Geomorphology 31(1-4):181–216. doi:10.1016/S0169-55X(99)00078-1

Guzzetti F, Reichenbach P, Cardinali M, Galli M, Ardizzone F (2005) Probabilistic landslide hazard assessment at the basin scale. Geomorphology 72(1-4):272–299. doi:10.1016/j.geomorph.2005.06.002

Guzzetti F, Reichenbach P, Ardizzone F, Cardinali M, Galli M (2006) Estimating the quality of landslide susceptibility models. Geomorphology 81(1-2):166–184. doi:10.1016/j.geomorph.2006.04.007

Hansen MJ (1984) Landslide hazard analysis. In: Brundsden D, Prior DB (eds) Slope instability. Wiley, Chichester, pp 523–602

Irigaray C (1995) Movimientos de Ladera: Inventario, Análisis y Cartografía de la Susceptibilidad Mediante un Sistema de Información Geográfica. Aplicación a las Zonas de Colmenar (Málaga), Rute (Córdoba) y Montefrío (Granada). Unpublished PhD Thesis, Department of Civil Engineering, University of Granada, Spain, 578 pp

Irigaray C, Fernández T, El Hamdouni R, Chacón J (1999) Verification of landslide susceptibility mapping. A case study. Earth Surf Proc Land 24(6):537–544. doi:10-1002/(SICI)1096-9837(199906)24:6<537:AID-ESP965>3.0.CO;2-6

Irigaray C, Lamas F, El Hamdouni R, Fernández T, Chacón J (2000) The importance of the precipitation and the susceptibility of the slopes for the triggering of landslides along the roads. Nat Hazards 21(1):65–81. doi:10.1023/A:1008126113789

Irigaray C, Fernández T, El Hamdouni R, Chacón J (2007) Evaluation and validation of landslide-susceptibility maps obtained by a GIS matrix method: examples from the Betic Cordillera (southern Spain). Nat Hazards 41(1):61–79. doi:10.1007/s11069-006-9027-8

Jiménez-Perálvarez JD, Irigaray C, El Hamdouni R, Fernández T, Chacón J (2005) Rasgos geomorfológicos y movimientos de ladera en la cuenca alta del río Guadalfeo, sector Cádiar-Órgiva (Granada). In: Alonso E, Corominas J (eds) VI Simposio Nacional sobre Taludes y Laderas Inestables. Valencia, Spain, pp 891–902

Jiménez-Perálvarez JD, Irigaray C, El Hamdouni R, Chacón J (2009) Building models for automatic landslide-susceptibility analysis, mapping and validation in ArcGIS. Nat Hazards 50(3):571–590. doi:10.1007/s11069-008-9305-8

Junta de Andalucía (2005) Modelo Digital del Terreno de Andalucía. Consejería de Obras Públicas y Transportes, Consejería de Agricultura y Pesca, Consejería de Medio Ambiente. ISBN: 84-96329-34-8

Keller EA, Sanz de Galdeano C, Chacón J (1996) Tectonic geomorphology and earthquake hazard of Sierra Nevada, Southern Spain. In: Chacón J, Rosúa JL (eds) 1a Conferencia Internacional Sierra Nevada. Granada, pp 201–218

Köppen W (1936) Das geographische system der klimate. In: Köppen W, Geiger R (eds) Handbuch der klimatologie, 1C. Gebrüder borntraeger, Berlin, pp 44

Lang R (1915) Versuch einer exakten Klassifikation der Böden in klimatischer und geologischer Hinsicht. Int Mittig. f. Bodenkunde 5:312–346

Ortega M, Nieto F, Rodríguez J, López AC (1985) Mineralogía y estratigrafía de los sedimentos neógenos del corredor de la Alpujarra (Cordillera Bética, España). Bol Soc Esp Miner 8:307–318

Remondo J, González A, de Díaz Terán JR, Cendrero A, Fabbri A, Cheng CF (2003) Validation of landslide susceptibility maps: examples and applications from a case study in Northern Spain. Nat Hazards 30(3):437–449. doi:10.1023/B:NHAZ.0000007201.80743.fc

Ruiz Sinoga JD, Martinez Murillo JF (2009) Effects of soil surface components on soil hydrological behaviour in a dry Mediterranean environment (Southern Spain). Geomorphology 108(3-4):234–245. doi:10.1016/j.geomorph.2009.01.012

Soeters R, Van Westen JC (1996) Slope instability recognition, analysis, and zonation. In: Turner AK, Schuster RL (eds) Landslides: investigation and mitigation. National Academic Press. Washington D.C. Sp-Rep 247, pp 129–177

Thornes JB, Alcántara-Ayala I (1998) Modelling mass failure in a Mediterranean mountain environment: climatic, geological, topographical and erosional controls. Geomorphology 24(1):87–100. doi:10.1016/S0169-555X(97)00103-7

UNESCO Working Party On World Landslide Inventory (WP/WLI) (1993) A suggested method for describing the activity of a landslide. Bull Eng Geol Environ 47(1):53–57. doi:10.1007/BF02639593

UNESCO–A.I.G.I. (1976) Guide pour la préparation des cartes géotechiques. Paris, Presses Unesco, Sc. De la Terre n°15, 79p

Van Bemmelen RW (1927) Bijdrage tot de geologie der Betisch Ketens in de provincie Granada. PhD Thesis, University of Delft, 176 pp

Van Westen CJ (2000) The modelling of landslide hazards using GIS. Surv Geophys 21(2-3):241–255. doi:10.1023/A:1006794127521

Van Westen CJ, Rengers N, Terlien MTJ, Soeters R (1997) Prediction of the occurrence of slope instability phenomena through GIS-based hazard zonation. Int J Earth Sci (Geologische Rundschau) 86(2):404–414. doi:10.1007/s005310050149

Varnes DJ (1978) Slope movements types and processes. In: Schuster RL, Kizek RJ (eds) Landslides: analysis and control. National Academy of Sciences, Washington DC, Special report 176(2), pp 11–33

Varnes DJ (1984) Landslide hazard zonation: a review of principles and practice. Natural hazards 3. Commission on Landslides of the IAEG, UNESCO, Paris

Rank in Category: Bulletin of Engineering Geology and the Environmen...

Journal Ranking

For **2011**, the journal **Bulletin of Engineering Geology and the Environmen...** has an Impact Factor of **0.667**.

This table shows the ranking of this journal in its subject categories based on Impact Factor.

Category Name	Total Journals in Category	Journal Rank in Category	Quartile in Category
ENGINEERING, ENVIRONMENTAL	45	39	Q4
ENGINEERING, GEOLOGICAL	30	19	Q3
GEOSCIENCES, MULTIDISCIPLINARY	170	141	Q4

Category Box Plot

For **2011**, the journal **Bulletin of Engineering Geology and the Environmen...** has an Impact Factor of **0.667**.

This is a box plot of the subject category or categories to which the journal has been assigned. It provides information about the distribution of journals based on Impact Factor values. It shows median, 25th and 75th percentiles, and the extreme values of the distribution.

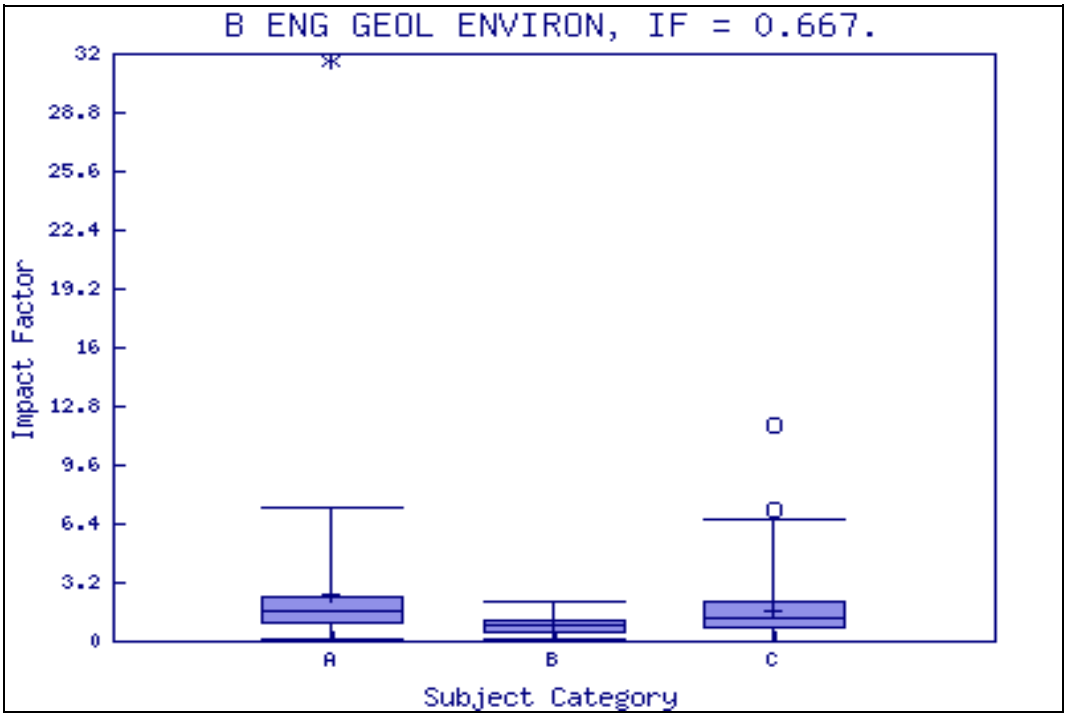

Key

A - ENGINEERING, ENVIRONMENTAL

B - ENGINEERING, GEOLOGICAL

C - GEOSCIENCES, MULTIDISCIPLINARY

Journal: Bulletin of Engineering Geology and the Environment

Mark	Journal Title	ISSN	Total Cites	Impact Factor	5-Year Impact Factor	Immediacy Index	Citable Items	Cited Half-life	Citing Half-life
☐	B ENG GEOL ENVIRON	1435-9529	436	0.667	0.826	0.059	68	5.9	>10.0

Cited Journal | Citing Journal | Source Data | Journal Self Cites

CITED JOURNAL DATA | CITING JOURNAL DATA | IMPACT FACTOR TREND | RELATED JOURNALS

Journal Information

Full Journal Title: Bulletin of Engineering Geology and the Environment
ISO Abbrev. Title: Bull. Eng. Geol. Environ.
JCR Abbrev. Title: B ENG GEOL ENVIRON
ISSN: 1435-9529
Issues/Year: 4
Language: ENGLISH
Journal Country/Territory: GERMANY
Publisher: SPRINGER HEIDELBERG
Publisher Address: TIERGARTENSTRASSE 17, D-69121 HEIDELBERG, GERMANY
Subject Categories: ENGINEERING, ENVIRONMENTAL
SCOPE NOTE | VIEW JOURNAL SUMMARY LIST | VIEW CATEGORY DATA
ENGINEERING, GEOLOGICAL SCOPE NOTE | VIEW JOURNAL SUMMARY LIST | VIEW CATEGORY DATA
GEOSCIENCES, MULTIDISCIPLINARY
SCOPE NOTE | VIEW JOURNAL SUMMARY LIST | VIEW CATEGORY DATA

***Eigenfactor*® Metrics**
***Eigenfactor*® Score** 0.00160
***Article Influence*® Score** 0.329

Journal Rank in Categories: JOURNAL RANKING

Journal Impact Factor

Cites in 2011 to items published in: 2010 = 21, 2009 = 55, Sum: 76
Number of items published in: 2010 = 60, 2009 = 54, Sum: 114

Calculation: Cites to recent items 76 = **0.667**
Number of recent items 114

5-Year Journal Impact Factor

Cites in {2011} to items published in:	2010 =	21	Number of items published in:	2010 =	60
	2009 =	55		2009 =	54
	2008 =	50		2008 =	68
	2007 =	42		2007 =	49
	2006 =	51		2006 =	34
	Sum:	219		Sum:	265

Calculation: Cites to recent items 219 = **0.826**
Number of recent items 265

Journal Self Cites

The tables show the contribution of the journal's self cites to its impact factor. This information is also represented in the cited journal graph.

Total Cites	436
Cites to Years Used in Impact Factor Calculation	76
Impact Factor	0.667

Self Cites	37 (8% of 436)
Self Cites to Years Used in Impact Factor Calculation	7 (9% of 76)
Impact Factor without Self Cites	0.605

Journal Immediacy Index

Cites in 2011 to items published in 2011 = 4
Number of items published in 2011 = 68
Calculation: Cites to current items 4 = **0.059**
Number of current items 68

Journal Cited Half-Life

The cited half-life for the journal is the median age of its items cited in the current JCR year. Half of the citations to the journal are to items published within the cited half-life.
Cited Half-Life: 5.9 years

Breakdown of the citations ***to the journal*** by the cumulative percent of 2011 cites to items published in the following years:

Cited Year	2011	2010	2009	2008	2007	2006	2005	2004	2003	2002	2001-all
# Cites from 2011	4	21	55	50	42	51	31	22	23	19	118
Cumulative %	0.92	5.73	18.35	29.82	39.45	51.15	58.26	63.30	68.58	72.94	100

Cited Half-Life Calculations:
The cited half-life calculation finds the number of publication years from the current JCR year that account for 50% of citations received by the journal. Read help for more information on the calculation.

Cited Journal Graph

Click here for Cited Journal data table

This graph shows the distribution by cited year of citations to items published in the journal B ENG GEOL ENVIRON.
Citations to the journal (per cited year)

- The white/grey division indicates the cited half-life (if < 10.0). Half of the journal's cited items were published more recently than the cited half-life.

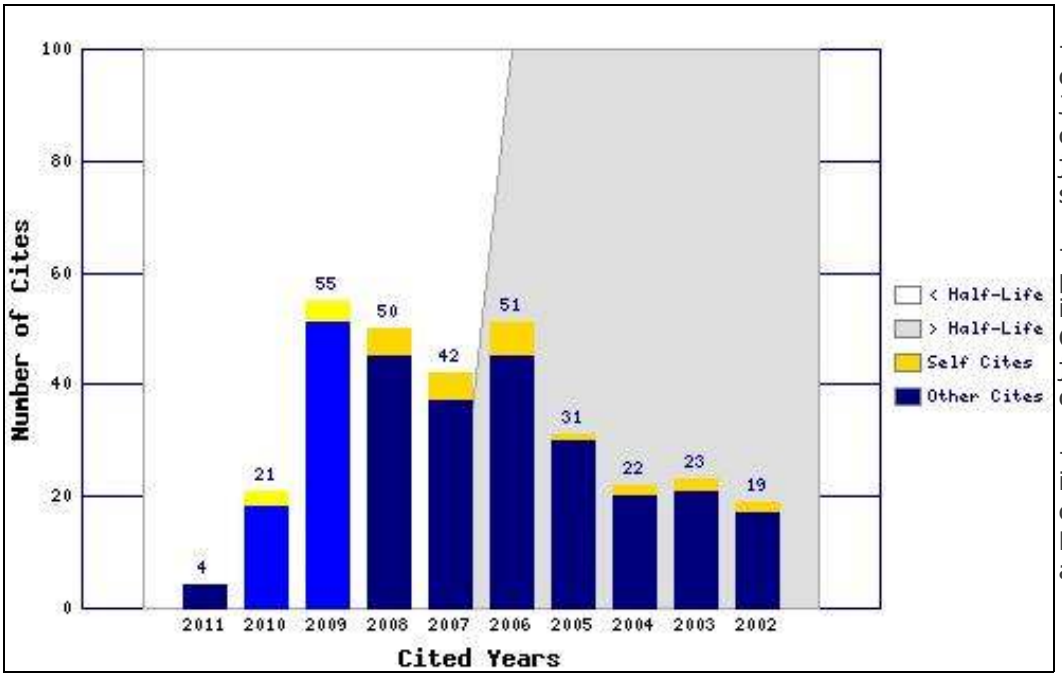

- The top (gold) portion of each column indicates Journal Self Citations: citations to items in the journal from items in the same journal.

- The bottom (blue) portion of each column indicates Non-Self Citations: citations to the journal from items in other journals.

- The two lighter columns indicate citations used to calculate the Impact Factor (always the 2nd and 3rd columns).

Journal Citing Half-Life

The citing half-life for the journal is the median age of the items the journal cited in the current JCR year. Half of the citations in the journal are to items published within the citing half-life.

Citing Half-Life: >10.0 years

Breakdown of the citations ***from the journal*** by the cumulative percent of 2011 cites to items published in the following years:

Cited Year	2011	2010	2009	2008	2007	2006	2005	2004	2003	2002	2001-all
# Cites from 2011	2	32	91	85	98	105	96	101	115	71	1136
Cumulative %	0.10	1.76	6.47	10.87	15.94	21.38	26.35	31.57	37.53	41.20	100

Citing Half-Life Calculations:
The citing half-life calculation finds the number of publication years from the current JCR year that account for 50% of citations in the journal. Read help for more information on the calculation.

Citing Journal Graph

Click here for Citing Journal data table

This graph shows the distribution by cited year of citations from current-year items in the journal B ENG GEOL ENVIRON.

Citations from the journal (per cited year)

- The white/grey division indicates the citing half-life (if < 10.0). Half of the citations from the journal's current items are to items published more recently than the citing half-life.

- The top (gold) portion of each column indicates Journal Self-Citations: citations from items in the journal to items in the same journal.

- The bottom (blue) portion of each column indicates Non-Self Citations: citations from the journal to items in

other journals.

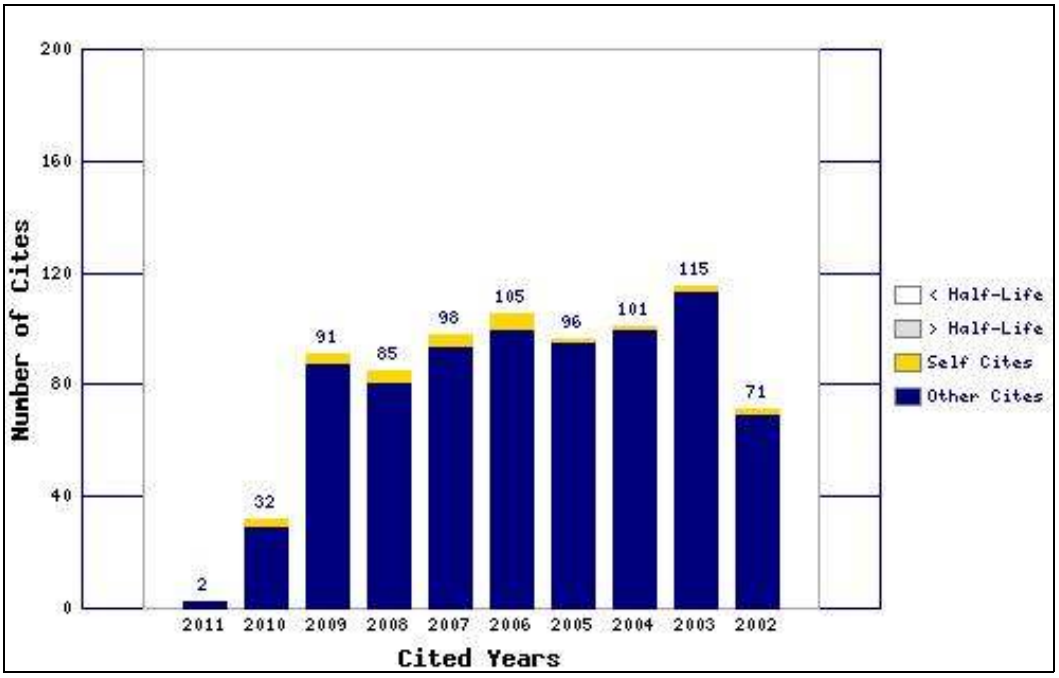

Journal Source Data

	Citable items			
	Articles	**Reviews**	**Combined**	**Other items**
Number in JCR year 2011 (A)	67	1	68	2
Number of references (B)	1897	34	1931	1.00
Ratio (B/A)	28.3	34.0	28.4	0.5

Bull Eng Geol Environ (2012) 71:569–578
DOI 10.1007/s10064-011-0414-3

ORIGINAL PAPER

Spatial stability of slope cuts in rock massifs using GIS technology and probabilistic analysis

C. Irigaray · R. El Hamdouni · J. D. Jiménez-Perálvarez · P. Fernández · J. Chacón

Received: 30 March 2011 / Accepted: 11 November 2011 / Published online: 17 January 2012

Abstract This paper presents a methodology for the stability analysis of cuts in rock slopes. A kinematic analysis of the different types of failure (planar, wedge, and toppling) is developed using GIS, following which a probabilistic analysis is made of the limit equilibrium in slopes where the conditions for kinematic failure are satisfied. The results were verified by comparing the evaluation against the observed stability conditions in 40 road cuts along 4 km of national road N-340, on the Mediterranean edge of Granada province (southern Spain). The validation analysis showed that for some 90% of the slopes studied there was a reasonable fit between the observed and evaluated stability, indicating the proposed methodology is suitable for the preliminary analysis of the stability conditions on rock slopes.

Keywords Rock slopes · Kinematic analysis · Safety factor · Failure probability · GIS

Résumé Le littoral entre Radès et Ezzahra, au nord-est de la Tunisie, a souffert de l'érosion pendant une forte tempête en 1981. En conséquence, entre 1985 et 1988 un brise-lames a été construit à Radès et deux brise-lames à Ezzahra. L'article présente une étude de l'efficacité de ces structures et considère les autres facteurs qui contrôlent les processus d'accrétion et d'érosion du littoral.

Mots clés Brise-lames · Erosion littorale · Accrétion littorale · Radès-Ezzahra · Tunisie

C. Irigaray (✉) · R. El Hamdouni · J. D. Jiménez-Perálvarez · P. Fernández · J. Chacón
Department of Civil Engineering, ETSICCP, University of Granada, Campus Fuentenueva s/n, Granada 18071, Spain
e-mail: clemente@ugr.es

Introduction

Stability assessments of rock slopes involving civil works are generally preceded by a kinematic analysis which forms the basis for the selection of cut slopes for further assessment of the factor of safety (Hoek and Bray 1981; Norrish and Wyllie 1996). A kinematic analysis is a geometrical method developed using stereographic projections. It can assist in the determination of likely failure modes, the geometrical relationships between discontinuities and the relevant friction angles, and has been reported by several authors (Hoek and Bray 1981; Yoon et al. 2002).

According to the equilibrium-limit method, the failure of a rock mass occurs above a discontinuity when the shear stress surpasses the shear strength of this surface. Generally, this type of analysis is made by the deterministic calculation of the factor of safety (Goodman and Bray 1976; Kumsar et al. 2000; Hoek 2007). However, the uncertainty and/or variability associated with the geotechnical properties of materials hampers the selection of the appropriate values needed for this type of analysis and gave rise to the development of probabilistic methods. Some authors have proposed substituting the use of the standard safety factor, FS, for the reliability index, RI, (e.g Christian et al. 1994) or the probability of failure, PF (Hoek 2007).

Numerous authors have used the equilibrium-limit method for the stability analysis of rock slopes, both from the deterministic standpoint (Sarma 1979; Warburton 1981) as well as the probabilistic approach (Priest and Brown 1983). However, this method has the limitation that the failure mode must be known before it can be applied; that is, the method cannot recognize the failure mode without the help of a prior kinematic analysis (Kim et al. 2004).

The spectacular increase in the availability of computers in recent years and the development of GIS have provided powerful tools to analyse spatial information. GIS has been widely used to analyse stability against slope movements in general (Carrara et al. 1991; Chacón et al. 1996, 2006; Chacón and Corominas 2003; Irigaray et al. 2007), but there are fewer examples of its use in rock slopes (Gokceoglu et al. 2000; Irigaray et al. 2003, 2010; Günther et al. 2004; Kim et al. 2004; Aksoy and Ercanoglu 2007). This paper presents a methodology incorporating ArcGIS 9.3 (ESRI 2009). It was validated by stability analyses for different types of failure controlled by the discontinuities in rock masses at the Mediterranean edge of the province of Granada (southern Spain).

Location of the study area

The study area is located on the coast of Granada (southern Spain) 15–20 km east of the city of Motril (Fig. 1). Geologically, it belongs to the Alpujarride Complex of the Internal Zones of the Betic Cordillera. It is covered by the carbonate materials of the Murtas Unit of Triassic age (Aldaya 1981), although in places the underlying Permo-Triassic phyllites crop out.

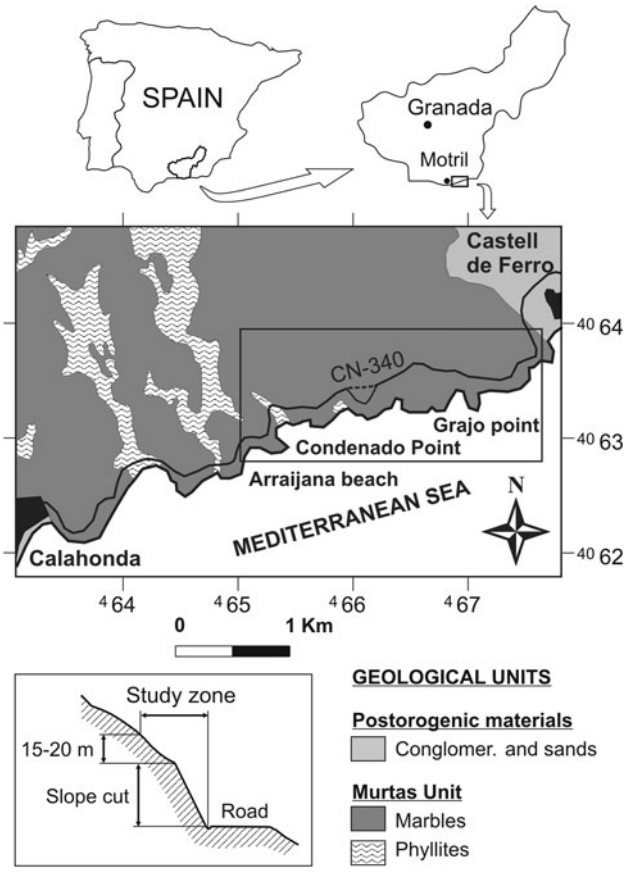

Fig. 1 Location of the study area

Thirteen rock slopes along national highway N-340 (between the Arraijana beach and Castell de Ferro) were selected for study, based on their geological and structural features. The study was limited to the surface area between the highway and a height of between 15 and 20 m above the road. Some of these slopes were sub-divided into sections, either because the ground plan of the slope was curved or because they included significant lithological or structural differences, such that a total of 40 slope units were studied. Figure 2 is an example of one of the studied slope units.

The meteorological records show the maximum temperature in July and August is some 26–27°C while in February the minimum is some 13°C. The mean annual rainfall is 486 mm; the precipitation peaking in March (monthly mean of 69 mm) and December (90 mm) while in July it is as little as 1 mm.

Data collection

Scan line surveys were made of representative slopes, following Hoek and Bray (1981), and Hudson and Priest 1983). A total of 2,330 m of scanline were undertaken for 740 analysed discontinuities and their geomechanical parameters measured, including spacing, resistance to compression, weathering, presence of water, etc. (Irigaray et al. 2003). The tilt test was used to measure the angle of friction (Bruce et al. 1989; Franklin and Dusseault 1989; Barton 2008). Cohesion was not measured but was estimated based on information published on similar rocks (Hoek and Bray 1981; Goodman 1989; Waltham 1999).

Some of the data needed for the analysis were obtained using a Digital Elevation Model (with a 2 × 2 m cell size) and ArcGIS 9.3 (ESRI 2009). The topographic and cartographic information used was prepared by Granada Province Council in 1998 at a scale of 1:2,000.

Table 1 shows the general characteristics and the mean geomechanical parameters for one of the slopes studied. All the information acquired was implemented in the Geographic Information System ArcGIS 9.3 (ESRI 2009).

Methodology and results

Four sets of discontinuities were identified in each of the slope profiles and representative values of the geomechanical properties established. Stereographic projection was used (DIPS 5.0) to identify all the possible intersections between the sets of discontinuities present in each slope.

Fig. 2 Marble slope in the national road N-340 between Calahonda and Castell de Ferro (Granada, Spain)

Table 1 General characteristics and mean geomechanical parameters of the slope T1-a

Mean values of discontinuities (85 measurements):				
Set	1	2	3	4
Dip	68°	53°	33°	37°
Dip direction	273°	233°	137°	332°
Spacing (m)	0.1	0.1	0.3	0.2
Continuity	Sub-continuous	Not continuous	Continuous	Not continuous
Roughness	Slightly rough	Smooth	Slightly rough	Slightly rough
Infilling	No	Clay	Calcite	No
Aperture (mm)	0.1–1	0.1–1	>5	0.1–1
Weathering	Slightly weathered	Slightly weathered	Slightly weathered	Slightly weathered
Groundwater	Dry	Dry	Dry	Dry
Cohesion (kPa)	0	10	50	40
Friction angle (°)	33	32	33	36

Slope unit: T1-a. Excavation method: normal blasting. Maximum altitude: 12.5 m. Length: 110 m. Strike: N330°. Dip: 80°. Shape: rectilinear. Lithology: limestone-dolomitic marbles with alternating clear white and dark ones from centimetres to decimetres in thickness. Age: Triassic. Support measures: None. Breaks visible: formation of several decimetric wedges with low risk of falling. Uniaxial compressive strength: 37 MPa. Unit weight of rock: 26 kN/m^3

The stability conditions in the rock masses were analysed at two different stages (Goodman and Bray 1976; Hoek and Bray 1981; Goodman 1989; Norrish and Wyllie 1996). First, a kinematic analysis was made to determine the likelihood of planar, wedge, and/or toppling failure using GIS ArcGIS 9.3 (ESRI 2009). Where potential failure was identified, the factor of safety (FS) and probability of failure (PF) were determined using ROCPLANE 2.0 and SWEDGE 5.0 (Rocscience 2009b, c).

Kinematic analysis

The kinematic conditions for planar, wedge and toppling failure are recorded along the route corridor (Fig. 3). The slopes that present a greater extension of the zones with geometric instability are T8-c, T-7b, and T-8a, with values >20%. The slopes T-2a, T-7c, T-7d, T-7g, T8-g2, T9-1, T9-2, T11-a, and T13 presented no potential geometric instability (Fig. 3).

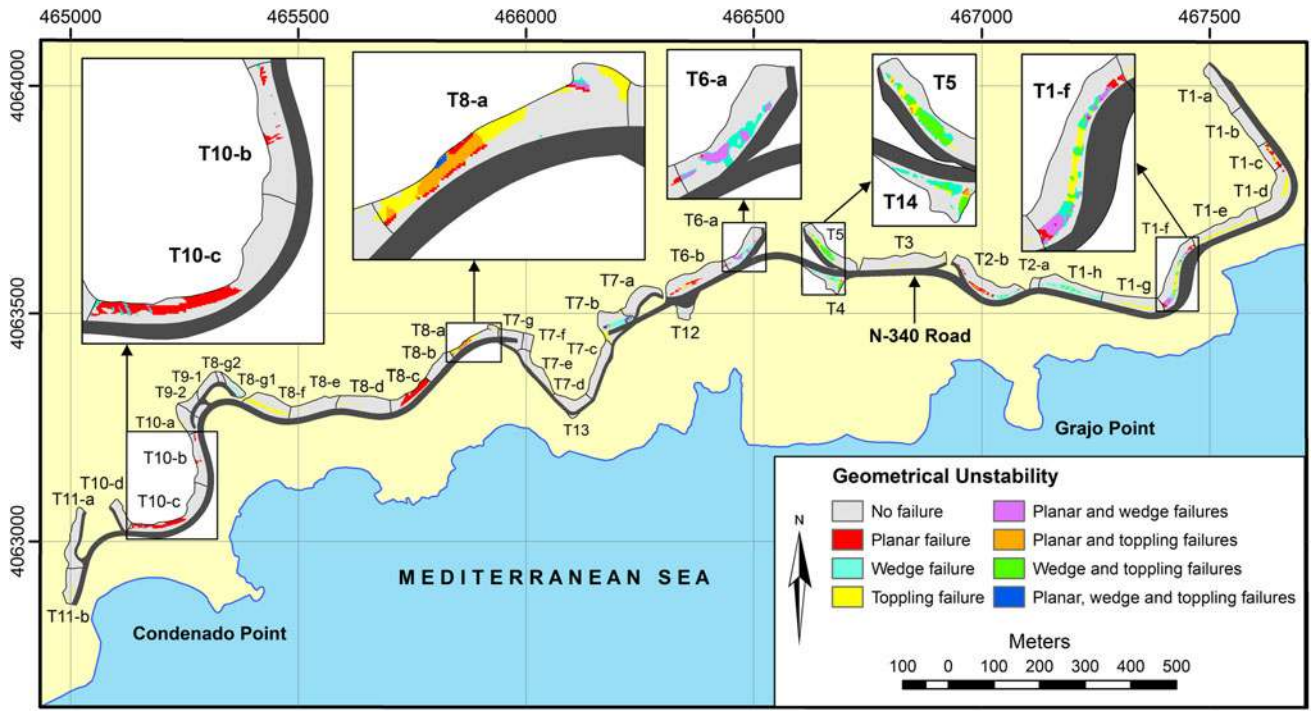

Fig. 3 Map of kinematic conditions for the planar, wedge, and toppling failure

Safety factor and failure probability

Factors of safety were established using limit-equilibrium analysis (Kovári and Fritz 1975; Hoek 2007), based on the parameters given in Tables 2, 3 and 4. In addition, a sensitivity analysis was made in order to determine the influence of the various parameters on the value of the calculated factor of safety. This type of analysis involves the application of the theory of probability to the risk evaluation (Harr 1987; Pine 1992) and provides a medium factor of safety (FS) as well as a probability of failure (PF). The results are given in Table 5.

The results are shown for the calculation of the safety factor by a probabilistic analysis for the cases of planar and wedge failure, made by the programs ROCPLANE 2.0 and SWEDGE 5.0, respectively (Rocscience 2009b, c). The analysis was made in all those slopes where the kinematic analysis indicated pixels that fulfilled the structural conditions of planar or wedge failure.

Planar failure

In the general case, the calculation of safety factor for planar failure of the slope is determined by the following equation (Norrish and Wyllie 1996; Hoek 2007):

$$FS=\frac{cA+\left(W\left(\cos\psi_p-\eta\sin\psi_p\right)-U-V\sin\psi_p+T\cos\theta\right)\tan\phi}{W\left(\sin\psi_p+\eta\cos\psi_p\right)+V\cos\psi_p-T\sin\theta}$$

where FS = factor of safety against sliding along a sheet joint; c = cohesive strength along a sliding surface; A = base area of wedge; W = weight of rock wedge resting on the failure surface; ψ_p = angle of failure surface, measured from horizontal; η = seismic coefficient; U = uplift force due to water pressure on failure surface; V = horizontal force due to water in tension crack (if present); T = force applied by the anchor system (if present); θ = inclination of the anchor, anti-clockwise from normal; ϕ = friction angle of sliding surface.

To determine the input data used for calculating the safety factor for the planar failure by ROCPLANE 2.0 (Rocscience 2009a) the following has been taken into account:

(a) *Geometry and weight* The slopes had no bench and in general had a rather uniform dip, so that the overall slope angle was considered fixed over its entirety. The failure planes were determined from prior kinematic analysis and appear to be almost smooth; thus the waviness angle is considered equal to 0. The overall slope height is considered fixed for the entire extension of the slope based on direct measurement in the field. The slope of the upper face corresponds to the angle of the natural slope from the DEM (Digital Elevation Model), and, given that it can present a certain variability over the slope, it was considered to be a random variable with a normal distribution and a

Table 2 Mean values of the input data used to calculate the probabilistic factor of safety for planar failure

Cut slope ID	Slope			Failure plane		Upper face	Strength	
	Angle (°)	Height (m)	Unit weight (kN/m^3)	No set	Angle (°)	Angle (°)	c (kPa)	ø (°)
T1-a	80	12.5	27	4	37	34	40	36
T1-b	75	12	27	4	43	35	50	30
T1-c	77	15	27	2	43	32	10	30
T1-d	75	15	26	3	61	33	30	34
T1-f	73	26	26	4	44	32	150	35
T1-h	72	29	26	4	62	33	120	34
T2-b	72	20	26	1	62	30	40	32
T4	69	23	26	3	61	34	40	37
T5	65	25	26	1	54	30	10	30
T6-a	67	15	27	4	41	34	40	37
T6-b	70	19	26	4	41	30	60	30
T7-b	68	20	26	4	46	33	5	36
T8-a	65	14	27	4	41	30	5	34
T8-c	62	18	26	4	38	28	5	36
T10-b	68	8	26	3	40	34	150	30
T10-c	46	12	26	4	43	34	20	32

Table 3 Mean values of the input data used to calculate the probabilistic factor of safety for wedge failure

Cut slope ID	Upper face		Slope face		Slope height (m)	Slope length (m)	Unit weight (kN/m^3)
	Dip (°)	DipDir (°)	Dip (°)	DipDir (°)			
T1-a	34	046	80	060	12.5	110	27
T1-b	35	053	75	060	12	95	27
T1-f	32	115	73	125	26	146	26
T1-h	33	200	72	200	29	140	26
T2-b	30	130	72	160	20	90	26
T4	19	285	69	003	16	80	26
T5	30	235	65	225	25	115	26
T6-a	41	115	67	125	15	100	27
T7-b	33	205	68	175	20	75	26
T8-a	30	155	65	155	14	120	27
T8-f	25	217	71	176	17	100	27
T8-g1	35	300	52	310	13	60	27
T10-b	34	62	68	72	8	113	26
T10-c	34	180	46	180	12	85	26
T12	24	189	52	359	6	40	26

standard deviation of 5°. The specific weight of the rock was determined from typical values in the literature (Farmer 1968; Goodman 1989; Waltham 1999). In field observations, no tension cracks were located; however, given the possibility that they could exist and that they were inadvertently overlooked, two situations were considered: without tension cracks and with tension cracks. In the latter, vertical tension cracks were considered with the FS location.

(b) *Water pressure* From field observations, the slopes appeared to be in a dry state (Irigaray et al. 2003). The carbonate nature of the materials (marbles) as well as their structural characteristics indicated drained conditions in all cases hence the water pressure was assumed to be nil.

(c) *External and seismic forces* In the slopes studied, no type of outer reinforcement was used and therefore in this section only seismic force is considered. Based on the Seismic-Resistance Construction Norm of Spain

Table 4 Mean values of the input data of discontinuities used to calculate the probabilistic factor of safety for wedge failure

Cut slope ID	Sets	Joint 1				Joint 2			
		Dip (°)	DipDir (°)	c (kPa)	ϕ (°)	Dip (°)	DipDir (°)	c (kPa)	ϕ (°)
T1-a	1∩4	68	273	0	33	37	332	40	36
T1-b	2∩3	42	125	0	35	73	25	150	29
T1-f	3∩4	68	051	150	34	44	140	150	35
T1-h	1–4	56	259	150	31	62	142	120	34
T2-b	1–4	62	223	40	32	52	115	20	35
T4	2–3	80	280	15	37	61	062	40	37
T5	1–4	54	277	10	30	73	146	5	35
T6-a	3–4	70	68	50	36	41	150	40	37
T7-b	3–4	74	056	150	36	46	138	5	36
T8-a	1–4	85	026	5	34	41	126	5	34
T8-f	1–4	75	025	10	36	38	117	30	36
T8-g1	1–2	88	244	10	35	58	286	50	36
T10-b	2–3	62	351	10	32	54	051	150	30
T10-c	1–4	63	276	70	34	43	172	20	32
T12	3–4	77	258	150	31	47	298	10	32

Table 5 Mean factor of safety (FS) and probability of failure (PF) obtained into the ROCPLANE and SWEDGE analysis

Cut slope ID	ROCPLANE analysis				SWEDGE analysis	
	Without tension crack		With tension crack			
	FS	PF (%)	FS	PF (%)	FS	PF (%)
T1-a	1.23	7	1.01	45	5.91	0
T1-b	1.44	1	1.46	10	4.94	0
T1-c	0.59	100	0.55	100	–	–
T1-d	0.92	63	0.79	87	–	–
T1-f	1.67	0	1.31	0	2.63	0
T1-h	2.10	0	1.83	0	2.76	0
T2-b	1.13	29	1.00	50	1.21	9
T4	1.25	18	1.14	30	2.68	0
T5	0.48	100	0.46	100	1.22	6
T6-a	1.17	27	0.98	53	1.88	0
T6-b	1.24	15	1.01	48	–	–
T7-b	0.60	100	0.58	100	0.70	100
T8-a	0.68	100	0.65	100	0.72	100
T8-c	0.78	100	0.76	100	–	–
T8-f	–	–	–	–	5.33	0
T8-g1	–	–	–	–	3.88	0
T10-b	4.36	0	3.03	0	17.28	0
T10-c	2.78	4	2.61	4	3.55	0
T12	–	–	–	–	19.01	0

NCSR-02 (Ministerio de Fomento 2002), the seismic coefficient of the study sector (town of Gualchos) is equal to 0.13 g.

(d) *Shear strength* The relationship between the shear strength (τ) of the failure plane and the normal stress (σ_n) acting on the plane is represented by the Mohr–Coulomb equation:

$$\tau = c + \sigma_n \tan \phi$$

where ϕ is the friction angle of the failure plane and c is the cohesion.

The friction angle of the discontinuities has been estimated from data measured directly in the field by the tilt test (Barton 1981; Franklin and Dusseault 1989). From

these results, and taking into account the data from the literature (Farmer 1968; Hoek and Bray 1981; Goodman 1989; Waltham 1999) a normal distribution was considered for this variable, with a standard deviation of 5°. No experimental data were available to determine the cohesion of the discontinuities for the study zone hence this parameter was estimated on the basis of information published for similar rocks (Farmer 1968; Hoek and Bray 1981; Goodman 1989; Waltham 1999). A normal truncated distribution was assumed with a minimum value of 0 kPa, a maximum equal to double the mean values, and a standard deviation of 10 kPa.

(e) S*ampling technique* The sampling technique used in the probabilistic analysis was the Latin Hypercube (Iman et al. 1980), which provides results comparable to those of the Monte Carlo technique (Harr 1987) but with fewer samples (Hoek 2007).

Table 2 shows the mean values of the input data used to calculate the probabilistic factor of safety for planar failure.

Wedge failure

In the case of wedge failure, the calculation of the safety factor is given below[1] (Kumsar et al. 2000): where FS = factor of safety; W = weight of the rock wedge resting on failure surfaces; i_a = intersection angle; η = seismic coefficient; β = inclination angle of a dynamic force ($\beta = 0$ for seismic forces); c = cohesive strength along the sliding surfaces; U_s = water force acting on the face of the slope (if present); U_t = water force acting on the upper part of the slope (if present); U_b = force caused by fluid pressure normal to each joint; A_1 and A_2 = joint surface areas; ϕ = friction angle; λ = wedge factor by Kovári and Fritz (1975):

$$\lambda = \frac{\cos\omega_1 + \cos\omega_2}{\sin(\omega_1 + \omega_2)}$$

where ω_1 and ω_2 are the angles between the surfaces of each joint with the vertical.

Taking into account the same considerations as in the analysis of the planar failure, in the probabilistic analysis for wedge failure neither benches, tension cracks, nor water pressure were considered. The Latin HyperCube sampling method was used.

Tables 3 and 4 show the mean values of these data for the talus that fulfil the kinematic conditions of wedge failure.

[1]

$$FS = \frac{[\lambda[W(\cos i_a - \eta\sin(i_a+\beta)) + U_s\sin i_a + U_t\cos i_a] - U_b]\tan\phi + c(A_1+A_2)}{W(\sin i_a + \eta\cos(i_a+\beta) - U_s\cos i_a + U_t\sin i_a}$$

Table 5 shows the FS and PF calculated for the different conditions studied in the slopes where the kinematic conditions were satisfied. The results show that

(a) The slopes that presented the greatest probability of failure, both for planar failure and wedge failure (FS < 1 and PF = 100%) were slopes T7-b and T8-a.
(b) Slopes T1-c and T8-c also presented the greatest probability of failure, but, in these, planar failure was geometrically possible.
(c) Slope T5 presented the maximum probability of planar failure, and a lower probability of wedge failure (FS = 1.22 and PF = 6%). However, the extension where the planar failure was geometrically possible was very reduced in this slope.
(d) Slopes T1-d, T2-b, T4, T6-b, T8-f, and T10-c could also present instability problems but with low probabilities of failure (maximum 63% in T1-d).
(e) The rest of the slopes presented very low or null probabilities of failure.

Validation of the results

With the aim of testing the validity of the results, a comparative analysis was made between the evaluation and field observation.

Table 6 shows the failures detected in the field, as well as the overall evaluation of the stability of the slopes studied. It also includes the results of the kinematic and equilibrium limit analyses.

Table 7 shows the failure categories for the 40 slopes. It can be seen that the mathematical analyses for 36 of the 40 slopes studied (90%) were generally consistent with the stability observed in the field. The five slopes directly observed as "unstable" were compatible with failure, both from the geometric and limit equilibrium analysis. In the ten slopes showing "stable" conditions, it was confirmed that failure kinematic or limit equilibrium conditions were not accomplished. The seven slopes directly observed as "rather unstable" included five slopes fulfilling all the failure requirements, one slope which showed the kinematic conditions for toppling failure and only one slope which did not satisfy geometric failure conditions. In the 18 slopes directly observed as "rather stable", only three of them were considered as failed using the proposed methodology while the remaining 15 slopes show various different stable conditions (Table 7).

Determination of the appropriate slopes for the talus

Prior to the design of an engineering work in a rock mass, it is important to determine a stable slope angle which is cost effective. To determine whether the slopes studied were

Table 6 Failures detected and overall evaluation of the stability of all the slopes studied

Cut slope ID	KF			PF (%)		Observed failures	Observed stability
	P	W	T	P	W		
T1-a	Y	Y	Y	7–45	0	Plane failure, falling blocks	Rather stable
T1-b	Y	Y	N	1–10	0	Plane failure, few wedge failures	Rather stable
T1-c	Y	N	Y	100	–	Plane failure, falling blocks	Rather unstable
T1-d	Y	N	Y	87	–	Falling blocks	Rather unstable
T1-e	N	N	Y	–	–	Small falling blocks	Rather stable
T1-f	Y	Y	Y	0	0	Small falling blocks	Rather stable
T1-g	N	N	Y	–	–	Small falling blocks	Rather stable
T1-h	Y	Y	Y	0	0	Small wedge failure	Rather stable
T2-a	N	N	N	–	–	No	Stable
T2-b	Y	Y	Y	29–50	9	Plane and wedge failures	Unstable
T3	N	N	Y	–	–	Small falling blocks	Rather stable
T4	Y	Y	Y	18–30	0	Plane failure, falling blocks	Rather unstable
T5	Y	Y	Y	100	6	Falling blocks, wedge failure	Unstable
T6-a	Y	Y	N	27–53	0	Plane failure	Rather unstable
T6-b	Y	N	Y	15–48	–	Plane failure	Rather unstable
T7-a	N	N	Y	–	–	Small blocks	Rather Stable
T7-b	Y	Y	Y	100	100	Large wedge failure	Unstable
T7-c	N	N	N	–	–	No	Stable
T7-d	N	N	N	–	–	No	Stable
T7-e	N	N	Y	–	–	Small falling blocks	Rather stable
T7-f	N	N	N	–	–	Falling blocks	Rather unstable
T7-g	N	N	N	–	–	No	Rather stable
T8-a	Y	Y	Y	100	100	Plane failure, falling blocks, wedge failure	Unstable
T8-b	N	N	N	–	–	No	Rather stable
T8-c	Y	N	N	100	–	Plane failure, falling blocks	Unstable
T8-d	N	N	Y	–	–	Falling blocks	Rather unstable
T8-e	N	N	Y	–	–	Falling blocks	Rather stable
T8-f	N	Y	Y	–	0	Falling blocks, wedge failure	Rather stable
T8-g1	N	Y	N	–	0	Small wedge failure	Rather stable
T8-g2	N	N	N	–	–	No	Stable
T9-1	N	N	N	–	–	No	Stable
T9-2	N	N	N	–	–	No	Stable
T10-a	N	N	Y	–	–	Small falling blocks	Rather stable
T10-b	Y	Y	N	0	0	Small falling blocks	Rather stable
T10-c	Y	Y	N	4	0	Small plane failure	Rather stable
T10-d	N	N	Y	–	–	No	Stable
T11-a	N	N	N	–	–	No	Stable
T11-b	N	N	Y	–	–	Small falling blocks	Rather stable
T12	N	Y	N	–	0	No	Stable
T13	N	N	N	–	–	No	Stable

KF Kinematic failure; *P* Planar failure; *W* Wedge failure; *T* Toppling failure; *Y* Yes; *N* No; *PF* Probability of failure

sufficiently stable, determinations were made of the slope angle which would give an FS against planar and wedge failure, of >1.5, assuming the remainder of the parameters considered in the equilibrium-limit analysis remained unchanged. Table 8 shows the recommended angles, which in some cases indicate a reduction in angle of some 20°. Where the recommended angles could not be achieved, whether for geometric or economic reasons, it is highly

Table 7 Distribution of the number of slopes that fulfil different conditions for failure and observed stability

Observed stability	Plane or wedge failure		Toppling failure	No kinematic conditions for failure
	LE	NLE		
Unstable (5)	5	0	0	0
Rather unstable (7)	5	0	1	1
Rather stable (18)	3	5	8	2
Stable (10)	0	1	1	8

LE Compatibility with failure according to the limit equilibrium analysis. No compatibility with failure according to the limit equilibrium analysis

Table 8 Actual slope angle (A) and recommended slope angle (α) for unstable slopes to reach a safety factor higher than 1.5

Cut slope ID	T1-c	T1-d	T2-b	T4	T5	T6-a	T6-b	T7-b	T8-a	T8-c
A (°)	77	75	72	69	65	67	70	68	65	62
α (°)	45	67	58	66	46	55	55	47	42	39

recommended that an adequate support of some outer reinforcement be applied (wire mesh, anchors, etc.).

Discussion and conclusions

The aim of the present work was to propose a methodology for analysing the stability conditions of rock slopes. It involves two stages:

1. A kinematic analysis of the different types of failure (planar, wedge, and toppling) using GIS.
2. A probabilistic analysis of the limit equilibrium in the slopes where the conditions of kinematic failure were satisfied.

The results were verified by the comparing the instability evaluation and the instability conditions observed on site.

In the case of the study area, situated on the national highway N-340 in southern Spain, the kinematic analysis indicated that 27 of the 40 slopes studied presented geometric conditions consistent with failure. Of these 27 slopes, 7 had safety factors lower than 1 for planar or toppling failure, of which 5 presented a probability of failure of 100% with the parameters estimated. The validation analysis showed that, overall, for 90% of the slopes studied there was a reasonable fit between the calculated and observed stability, indicating the methodology is useful for a preliminary analysis.

The main limitation of this type of analysis is the estimation of the parameters of the discontinuities, especially the friction and cohesion angle, particularly taking into account local conditions, as well as the climate and geomorphology. The results for the basic friction angles determined from tilt tests were corrected taking into account published experimental results on peak friction angle. More limitations were found in the selection of cohesion values, as it was not possible to make direct measurements between discontinuity planes.

The methodology proposed should be used in combination with other sources of information and analysis methods, and only in the preliminary phases of the design and planning of engineering works. However, in these preliminary phases, GIS constitutes a quick, inexpensive and effective tool for analysing the spatial stability of natural and cut slopes, which can provide useful information when time and economic resources are limited and indicate areas where more specific investigations and analyses should be focussed.

Acknowledgments This research was supported by projects CGL2008-04854 funded by the Ministry of Science and Education of Spain, and Excellence Project P06-RNM-02125, funded by the Regional Government. Rainfall dates have been supplied by the National Meteorological Institute of Spain. It was developed in the RNM-121 Research Group funded by the Andalusian Research Plan.

References

Aksoy H, Ercanoglu M (2007) Fuzzified kinematic analysis of discontinuity-controlled rock slope instabilities. Eng Geol 89:206–219

Aldaya F (1981) Mapa geológico de España, E. 1:50.000, 1056 (Albuñol). IGME, Madrid

Barton N (1981) Shear strength investigation for surface mining. In: 3rd International Conference on stability surface mining, Vancouver

Barton N (2008) Shear strength of rockfill, interfaces and rock joints, and their points of contact in rock dump design. In: Fourie A (ed) Rock dumps. Australian Centre for Geomechanics, Perth

Bruce IG, Cruden DM, Eaton TM (1989) Use of a tilting table to determine the basic friction angle of hard rock samples. Can Geotech J 26(3):474–479

Carrara A, Cardinali M, Detti R, Guzzetti F, Pasqui V, Reichenbach P (1991) GIS techniques and statistical models in evaluating landslide hazard. Earth Surf Proc Land 16:427–445

Chacón J, Corominas J (2003) Special issue on landslides and GIS. Nat Hazards 30(3):263–512

Chacón J, Irigaray C, El Hamdouni R, Fernández T (1996) From the inventory to the risk analysis: improvements to a large scale G.I.S. method. In: Chacón J, Irigaray C, Fernández T (eds) Landslides. Balkema, Rotterdam, pp 335–342

Chacón J, Irigaray C, Fernández T, El Hamdouni R (2006) Engineering geology maps: landslides and geographical information systems. Bull Eng Geol Environ 65:341–411

Christian JT, Ladd CC, Baecher GB (1994) Reliability applied to slope stability analysis. J Geotech Eng ASCE 120:2180–2207

ESRI (2009) ArcGIS Desktop 9.3. Environmental Systems Research Institute, Inc (ESRI) http://www.esri.com/

Farmer IW (1968) Engineering properties of rocks. Spon Ltd, London

Franklin JA, Dusseault MB (1989) Rock engineering. McGraw-Hill, New York

Gokceoglu C, Sonmez H, Ercanoglu M (2000) Discontinuity controlled probabilistic slope failure risk maps of the Altindag (settlement) region in Turkey. Eng Geol 55(4):277–296

Goodman RE (1989) Introduction to rock mechanics. Wiley, New York

Goodman RE, Bray JW (1976) Toppling of rock slopes. In: Proceedings of the specialty conference on rock engineering for foundations and slopes. American Society of Civil Engineers (ASCE), New York, pp 201–223

Günther A, Carstensen A, Pohl W (2004) Automated sliding susceptibility mapping of rock slopes. Nat Hazards Earth Syst Sci 4(1):95–102

Harr ME (1987) Reliability-based design in civil engineering. McGraw-Hill, New York

Hoek E (2007) Practical rock engineering. Rocscience-Hoek's Corner, USA http://www.rocscience.com/education/hoeks_corner

Hoek E, Bray JW (1981) Rock slope engineering. Institution of Mining and Metallurgy, London

Hudson JA, Priest SD (1983) Discontinuity frequency in rock masses. Int J Rock Mech Mining Sci Geomech Abst 20(2):73–89

Iman RL, Davenport JM, Zeigler DK (1980) Latin Hypercube sampling (a progam user's guide). Technical Report SAND 79-1473. Sandia Laboratories, Albuquerque

Irigaray C, Fernández T, Chacón J (2003) Preliminary rock-slope-susceptibility assessment using GIS and the SMR classification. Nat Hazards 30:309–324

Irigaray C, Fernández T, El Hamdouni R, Chacón J (2007) Evaluation and validation of landslide-susceptibility maps obtained by a GIS matrix method: examples from the Betic Cordillera (southern Spain). Nat Hazards 41:61–79

Irigaray C, El Hamdouni R, Jiménez-Perálvarez JD, Fernández P, Chacón J (2010) GIS application to a kinematics analysis and slope stability assessment of slope cuts on rock massifs along a national road in Southern Spain. In: Williams et al (eds) Geologically Active. Taylor and Francis Group, London, pp 1949–1957

Kim KS, Park HJ, Lee S, Woo I (2004) Geographic information system (GIS) based stability analysis of rock cut slope. Geosci J 8(4):391–400

Kovári K, Fritz P (1975) Stability analysis of rock slopes for plane and wedge failure with the aid of a programmable pocket calculator. In: 16th symposium Rock merchandise. ASCE, Minneapolis

Kumsar H, Aydan Ö, Ulusay R (2000) Dynamic and static stability assessment of rock slopes against wedge failures. Rock Mech Rock Eng 33:31–51

Ministerio de Fomento (2002) Real Decreto 997/2002, de 27 de septiembre, por el que se aprueba la norma de construcción sismorresistente: parte general y edificación (NCSR-02). BOE, n° 24, de 11 de octubre de 2002, pp 35898–35967

Norrish NI, Wyllie DC (1996) Rock slope stability analisys. In: Turner AK, Schuster RL (eds) Landslides, investigation and mitigation. National Research Council, Washington, pp 391–425

Pine RJ (1992) Risk analysis design applications in mining geomechanics. Trans Inst Min Metall 101:149–158

Priest SD, Brown ET (1983) Probabilistic stability analysis of variable rock slopes. Trans Inst Min Metall 92:1–12

Rocscience (2009a) Dips 5.0 graphical & statistical analysis of orientation data. © 2009 Rocscience Inc http://www.rocscience.com/

Rocscience (2009b) RocPlane 2.0 Planar sliding stability analysis for rock slopes. © 2009 Rocscience Inc http://www.rocscience.com/

Rocscience (2009c) Swedge 5.0 Surface Wedge Stability Software. © 2009 Rocscience Inc http://www.rocscience.com/

Sarma SK (1979) Stability analysis of embankments and slopes. J Geotech Eng ASCE 105:1511–1524

Waltham AC (1999) Foundations of engineering geology. E and FN Spon, London

Warburton PM (1981) Vector stability analysis of an arbitrary polyhedral rock block with any number of free faces. Int J Rock Mech Min 18(5):415–427

Yoon WS, Jeong UJ, Kim JH (2002) Kinematic analysis for sliding failure of multi-faced rock slopes. Eng Geol 67:51–61

Rank in Category: Bulletin of Engineering Geology and the Environmen...

Journal Ranking

For **2012**, the journal **Bulletin of Engineering Geology and the Environmen...** has an Impact Factor of **0.617**.

This table shows the ranking of this journal in its subject categories based on Impact Factor.

Category Name	Total Journals in Category	Journal Rank in Category	Quartile in Category
ENGINEERING, ENVIRONMENTAL	42	38	Q4
ENGINEERING, GEOLOGICAL	32	23	Q3
GEOSCIENCES, MULTIDISCIPLINARY	172	146	Q4

Category Box Plot

For **2012**, the journal **Bulletin of Engineering Geology and the Environmen...** has an Impact Factor of **0.617**.

This is a box plot of the subject category or categories to which the journal has been assigned. It provides information about the distribution of journals based on Impact Factor values. It shows median, 25th and 75th percentiles, and the extreme values of the distribution.

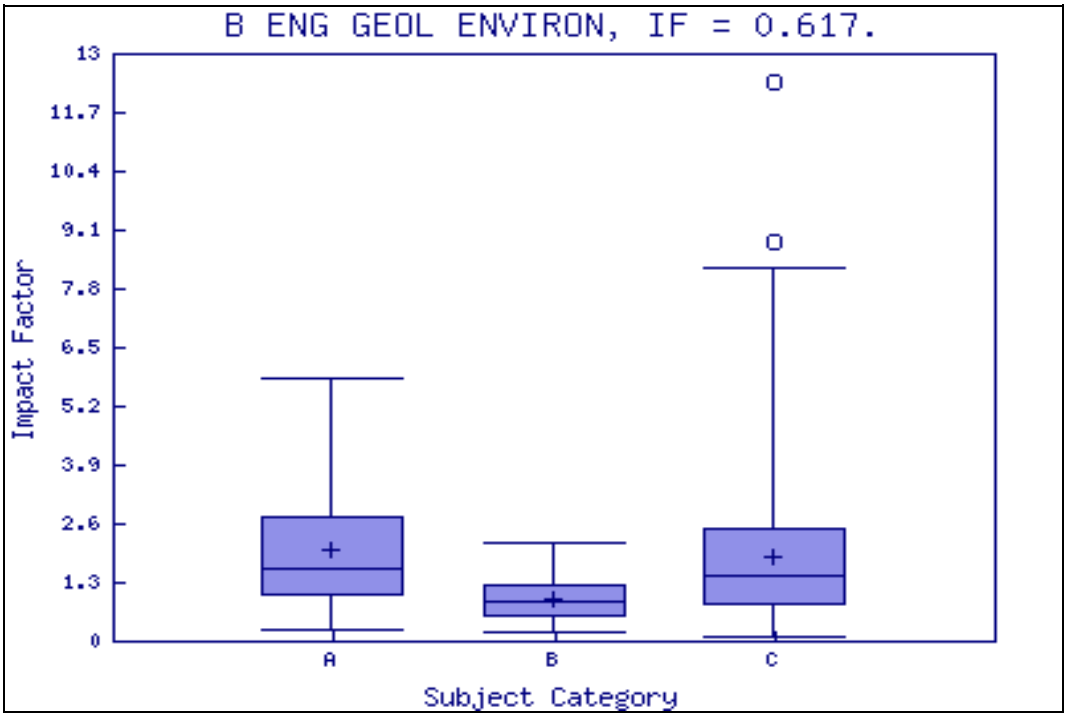

Key

A - ENGINEERING, ENVIRONMENTAL

B - ENGINEERING, GEOLOGICAL

C - GEOSCIENCES, MULTIDISCIPLINARY

Journal: Bulletin of Engineering Geology and the Environment

Mark	Journal Title	ISSN	Total Cites	Impact Factor	5-Year Impact Factor	Immediacy Index	Citable Items	Cited Half-life	Citing Half-life
☐	B ENG GEOL ENVIRON	1435-9529	672	0.617	0.963	0.191	68	6.4	>10.0

Cited Journal | Citing Journal | Source Data | Journal Self Cites

CITED JOURNAL DATA | CITING JOURNAL DATA | IMPACT FACTOR TREND | RELATED JOURNALS

Journal Information

Full Journal Title: Bulletin of Engineering Geology and the Environment
ISO Abbrev. Title: Bull. Eng. Geol. Environ.
JCR Abbrev. Title: B ENG GEOL ENVIRON
ISSN: 1435-9529
Issues/Year: 4
Language: ENGLISH
Journal Country/Territory: GERMANY
Publisher: SPRINGER HEIDELBERG
Publisher Address: TIERGARTENSTRASSE 17, D-69121 HEIDELBERG, GERMANY
Subject Categories: ENGINEERING, ENVIRONMENTAL
SCOPE NOTE | VIEW JOURNAL SUMMARY LIST | VIEW CATEGORY DATA
ENGINEERING, GEOLOGICAL SCOPE NOTE | VIEW JOURNAL SUMMARY LIST | VIEW CATEGORY DATA
GEOSCIENCES, MULTIDISCIPLINARY
SCOPE NOTE | VIEW JOURNAL SUMMARY LIST | VIEW CATEGORY DATA

***Eigenfactor*® Metrics**
***Eigenfactor*® Score** 0.00174
***Article Influence*® Score** 0.334

Journal Rank in Categories: JOURNAL RANKING

Journal Impact Factor

Cites in 2012 to items published in: 2011 = 30, 2010 = 49, Sum: 79
Number of items published in: 2011 = 68, 2010 = 60, Sum: 128

Calculation: Cites to recent items 79 = **0.617**
Number of recent items 128

5-Year Journal Impact Factor

Cites in {2012} to items published in:		Number of items published in:	
2011	=30	2011	=68
2010	=49	2010	=60
2009	=86	2009	=54
2008	=83	2008	=68
2007	=40	2007	=49
Sum:	288	Sum:	299

Calculation: Cites to recent items / Number of recent items = 288 / 299 = **0.963**

Journal Self Cites

The tables show the contribution of the journal's self cites to its impact factor. This information is also represented in the cited journal graph.

Total Cites	672
Cites to Years Used in Impact Factor Calculation	79
Impact Factor	0.617

Self Cites	45 (6% of 672)
Self Cites to Years Used in Impact Factor Calculation	9 (11% of 79)
Impact Factor without Self Cites	0.547

Journal Immediacy Index

Cites in 2012 to items published in 2012 = 13
Number of items published in 2012 = 68
Calculation: Cites to current items / Number of current items = 13 / 68 = **0.191**

Journal Cited Half-Life

The cited half-life for the journal is the median age of its items cited in the current JCR year. Half of the citations to the journal are to items published within the cited half-life.

Cited Half-Life: 6.4 years

Breakdown of the citations ***to the journal*** by the cumulative percent of 2012 cites to items published in the following years:

Cited Year	2012	2011	2010	2009	2008	2007	2006	2005	2004	2003	2002-all
# Cites from 2012	13	30	49	86	83	40	83	33	17	24	214
Cumulative %	1.93	6.40	13.69	26.49	38.84	44.79	57.14	62.05	64.58	68.15	100

Cited Half-Life Calculations:
The cited half-life calculation finds the number of publication years from the current JCR year that account for 50% of citations received by the journal. Read help for more information on the calculation.

Cited Journal Graph

Click here for Cited Journal data table

This graph shows the distribution by cited year of citations to items published in the journal B ENG GEOL ENVIRON.

Citations to the journal (per cited year)

- The white/grey division indicates the cited half-life (if < 10.0). Half of the journal's cited items were published more recently than the cited half-life.

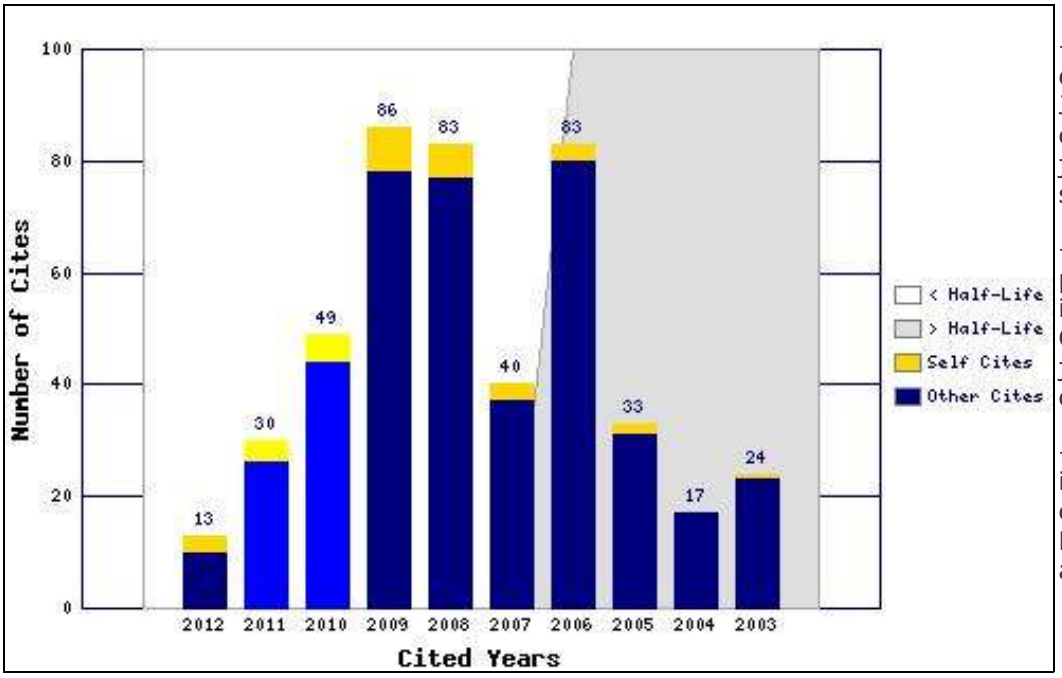

- The top (gold) portion of each column indicates Journal Self Citations: citations to items in the journal from items in the same journal.

- The bottom (blue) portion of each column indicates Non-Self Citations: citations to the journal from items in other journals.

- The two lighter columns indicate citations used to calculate the Impact Factor (always the 2nd and 3rd columns).

Journal Citing Half-Life

The citing half-life for the journal is the median age of the items the journal cited in the current JCR year. Half of the citations in the journal are to items published within the citing half-life.

Citing Half-Life: >10.0 years

Breakdown of the citations ***from the journal*** by the cumulative percent of 2012 cites to items published in the following years:

Cited Year	2012	2011	2010	2009	2008	2007	2006	2005	2004	2003	2002-all
# Cites from 2012	9	40	65	114	93	95	86	86	87	83	1503
Cumulative %	0.40	2.17	5.04	10.08	14.20	18.40	22.20	26.01	29.85	33.52	100

Citing Half-Life Calculations:
The citing half-life calculation finds the number of publication years from the current JCR year that account for 50% of citations in the journal. Read help for more information on the calculation.

Citing Journal Graph

Click here for Citing Journal data table

This graph shows the distribution by cited year of citations from current-year items in the journal B ENG GEOL ENVIRON.

Citations from the journal (per cited year)

- The white/grey division indicates the citing half-life (if < 10.0). Half of the citations from the journal's current items are to items published more recently than the citing half-life.

- The top (gold) portion of each column indicates Journal Self-Citations: citations from items in the journal to items in the same journal.

- The bottom (blue) portion of each column indicates Non-Self Citations: citations from the journal to items in

other journals.

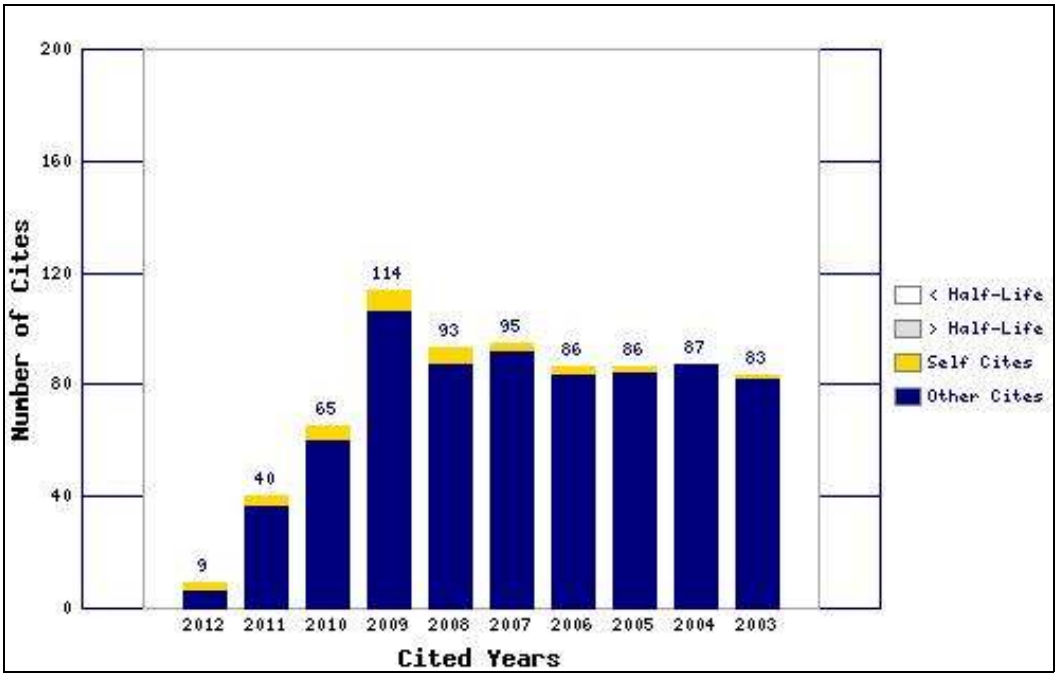

Journal Source Data

	Citable items			
	Articles	**Reviews**	**Combined**	**Other items**
Number in JCR year 2012 (A)	68	0	68	4
Number of references (B)	2202	0	2202	59.00
Ratio (B/A)	32.4	0.0	32.4	14.8